MONASH University

Control of Non-Synchronous Generating Plants to Improve Stability in Weak Grid Environments

Jessica Suzanne Peters
Bachelor of Commerce and Bachelor of Engineering (Honours)

A thesis submitted for the degree of Master of Engineering Science at
Monash University
Department of Electrical and Computer Systems Engineering

Copyright Notice

Abstract

Due to increasing concerns about global warming, renewable energy sources, such as wind and solar, are becoming more common. Synchronous generators are increasingly being replaced by non-synchronous generators, often interfaced to grid through inverters. With lower inertia from synchronous machines, this mixture of technology may cause problems in power system stability. The main aim of this research is to investigate how a power system can be stable with large amounts of renewable generation, and subsequently, lower inertia from synchronous machines.

The South Australian electricity network currently has one of the largest percentages of renewable energy in Australia. Within South Australia, rooftop solar generation was at 9% and wind generation was at 39% of the total electricity generated from 2016 to 2017 [1]. The network is also relatively isolated, with the Heywood Interconnector being the only AC link to Victoria and the rest of eastern Australia. To investigate the effect on stability of a network with mixed synchronous and non-synchronous generation, a simplified network model of the South Australian network has been developed in PSCAD as a case study.

The network is designed with a synchronous generator and an inverter representing the aggregated synchronous and asynchronous generation, the sizes of which can be varied to change the inverter penetration level. The Heywood Interconnector is also modelled and is connected to an external system representing eastern Australia.

Simulations are run at different inverter penetration levels using three different inverter control methods. These include algebraic control, PI control of active and reactive power, as well as PI control of active power and voltage. A single phase fault is introduced to the network in order to test the stability. As these initial results indicate a need for improvement to the inverter control, the PI controls for real and reactive power are tuned using the loop-shaping approach. After improvements are made to the inverter control, simulations show large improvements in the response of the network to disturbances.

The stability of the network is then tested at varying levels of inverter penetration in response to faults as well as the tripping of one of the parallel lines of the Heywood Interconnector. Increasing the power generated from the inverter relative to that generated from the synchronous generator does not have any negative impacts on stability. Very little difference is seen in terms of stability at the inverter penetration levels tested.

The disconnection of the Heywood Interconnector is also studied, isolating South Australia from the rest of the Australian network. Three different inverter penetrations levels are studied, with the levels of power being imported or exported from South Australia also being altered. Results show that increasing the amount of inverter-based generation has a positive effect on the stability of the network.

While this analysis has been done using a simplified version of the actual South Australian network and may be missing some of the complexities of the real network, these results indicate that increasing the amount of inverter-based generation within a network does not necessarily have a detrimental effect on stability, and may even improve it.

Declaration

This thesis contains no material which has been accepted for the award of any other degree or diploma at any university or equivalent institution and that, to the best of my knowledge and belief, this thesis contains no material previously published or written by another person, except where due reference is made in the text of the thesis.

Signature: .....

Print Name: .....

Date: .....

Acknowledgements

Firstly, I would like to acknowledge my supervisors for all their valuable advice as I was completing this research. I would like to thank my first supervisor, Dr Tadeusz Czaszejko, who took me on as his student. I would also like to thank Dr Behrooz Bahrani, who took over as my supervisor after Tadeusz retired. He has provided many helpful suggestions. I also thank Dr Tony Morton, for all the advice he gave as technical advisor.

I would like to thank the Faculty of Engineering at Monash University for granting me an ERLA scholarship, without which I would not have been able to complete this research. I also thank Professor Peter Wallace for his encouragement throughout my studies. Finally, I would like to thank my family for all their support as I completed my thesis.

Contents

List of Abbreviations

AEMO Australian Energy Market Operator

AGC Automatic Gerneration Control

DFIG Doubly-Fed Induction Generator

FCAS Frequency Control Ancillary Services

IGBT Insulated Gate Bipolar Transistor

NEM National Electricity Market

PI Proportional Integral

PLL Phase Locked Loop

PRBS Pseudo-Random Binary Sequence

PSS Power System Stabiliser

PU Per Unit

PWM Pulse-Width Modulation

ROCOF Rate Of Change Of Frequency

SCADA Supervisory Control And Data Aquisition

SCR Short Circuit Ratio

STATCOM STATic COMpensator

SVC Static VAR Compensator

THD Total Harmonic Distortion

1 Introduction

Due to increasing concerns about global warming, renewable energy sources such as wind and solar generation are becoming increasingly common within electricity networks around the world. Within South Australia, rooftop solar generation was at 9% and wind generation was at 39% of the total electricity generated from 2017 to 2017 [1]. More wind and solar farms have also been planned for the near future.

For many years, power systems have been primarily made up of synchronous generators, with the rotating masses of the machines providing inertia to the system. Renewable energy sources, on the other hand, are commonly non-synchronous and often use inverter interfaces to the grid. As these do not typically contribute any inertia to the system, increasing penetration of renewable energy sources in an electricity network can result in a weak grid.

As non-synchronous generation becomes a larger proportion of the total generated power within a network, this can have implications on the transient stability of the network. The lack of inertia and readily-available energy from the rotating masses of synchronous machines may lead to frequency and angle instability following disturbances. A mixed network of synchronous generators and non-synchronous generation may also adversely affect the ability of the synchronous machines to remain synchronised.

Research has shown that increasing inverter-based generation such as wind and solar also leads to reduced stability in the network [2–7]. In an attempt to improve on the stability issues in weak grids with lower inertia, research has emerged on inverters that can emulate the behaviour of synchronous machines, providing virtual inertia to the system [8–20]. These inverters use control systems that seek to capture the inertia and damping characteristics represented within the swing equations of synchronous machines.

The main aim of this research is to understand and investigate how a power system can be stable with large amounts of renewable energy generation, and subsequently, lower inertia from synchronous machines. The research focuses on simulating a network with both syn-

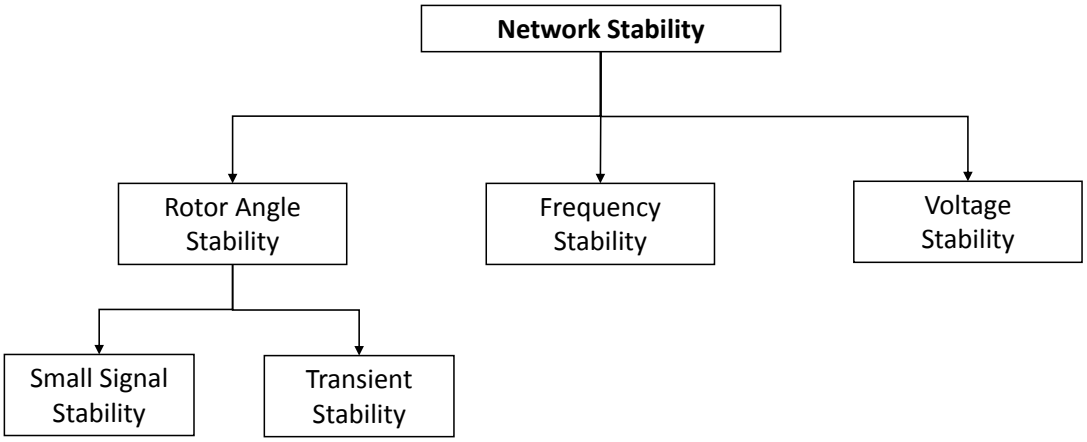

Figure 1.1 – Network stability components.

chronous generation and a large amount of inverter-based generation. This will be done using a simplified network model of the South Australian network. The effect of inverter penetration on stability will be investigated along with ways to improve the stability of the network, such as improving the control of inverters.

1.1 Network Stability

Before considering the impact of renewable generation on power system stability, the concepts of what makes a power system stable is first explored. For power systems to remain stable, it is important that they are able to remain in a state of equilibrium. They also must be able to return to this state of equilibrium after the occurrence of a disturbance [21, 22]. Instability can occur in a variety of ways including the loss of synchronisation of synchronous generators, oscillatory instability, or the excursion of frequency or voltage outside of their acceptable ranges.

The ability of a power system to remain stable under small disturbances, such as load changes, is referred to as small signal stability. These happen continually as the result of small variations in load and generation. Small signal stability problems tend to result mostly in oscillations due to inadequate damping [21]. A power system must also be able to handle large disturbances such as faults and short circuits, the loss of large generators or loads, or the loss of connection between two subsystems. The ability of the power system to maintain synchronism under these circumstances is known as transient stability [21]. Figure 1.1 summarises the different components of network stability that are required for a power system to remain stable. These are explained in more detail in the following subsections.

1.1.1 Rotor Angle Stability

It is important for synchronous machines to remain in synchronisation. Rotor angle stability refers to the ability of synchronous machines to remain synchronised after the occurrence of a disturbance [23]. In steady state conditions, the mechanical torque input into a generator is equal to the output electromagnetic torque. This results in a constant rotor speed and the generator is synchronised with the grid. If this equilibrium is disturbed, the rotor will either accelerate or decelerate and the machine may lose its synchronisation.

Rotor angle instability can either be oscillatory, due to a lack of damping torque, or non-oscillatory, due to the lack of synchronising torque [23]. Oscillations can be local problems in a small part of a power system, and usually involve a single power plant oscillating against the rest of the system [22]. These are known as local plant mode oscillations. Global oscillatory problems can also occur when a group of generators in one area swing against a group of generators in another. These oscillations are referred to as interarea mode oscillations [22].

1.1.2 Voltage Stability

A power network also needs to maintain voltage stability after a disturbance, with bus voltages being maintained at acceptable levels. The main cause of voltage instability is the unbalance in the demand supply of reactive power [23]. Some factors that can contribute to voltage instability are the strength of transmission lines, power transfer levels, load characteristics, generator reactive power capability limits, characteristics of reactive power compensation devices, poor coordination between control systems, and the actions of voltage control devices [23].

1.1.3 Frequency Stability

System frequency is determined by the power balance of a system. For a power system to maintain frequency stability, it must be able to maintain a steady state frequency within an acceptable margin after the occurrence of a disturbance causing a significant power imbalance between the generation and load. Frequency stability is particularly important as a drop in frequency could result in high amounts of magnetising currents in induction motors and transformers. Unstable frequency may also effect electric clocks and timing devices [21]. In extreme cases, frequency instability can lead to the tripping of generator or loads. It is common for frequency instability to occur after a large interconnected system is split into islands [23]. Frequency stability in a power system is influenced by the amount of inertia in the system as well as the actions of primary and secondary frequency control.

1.1.3.1 Inertia

Rotational inertia is the tendency of a rotating object to continue rotating at the same velocity unless torque is applied to it. The moment of inertia of an object is a measure of its resistance

to change. In relation to power systems, the higher the inertia the less sensitive the system frequency will be to load changes. In the absence of governors, the response of a synchronous machine to a load change is determined by inertia and damping constants. The mechanical part of a synchronous machine is modelled by the swing equation

$$J\ddot{\theta} = T_m - T_e - D_p\dot{\theta}, \tag{1.1}$$

where J is the moment of inertia of all parts rotating with the rotor, T_m is the mechanical torque, T_e is the electromagnetic torque, D_p is the damping factor, and θ is the rotor angle.

1.1.3.2 Primary Frequency Control

Primary frequency control is provided by the governors of synchronous machines. Load changes cause a change in the electrical torque outputs of synchronous generators. The mismatch between the electrical and mechanical torque results in speed, hence frequency, variations. Governors act in response to this mismatch to adjust generator turbine or gate positions, adjusting the mechanical torque and bringing the frequency back to its required range. Primary reserve is used to damp small deviations and occurs in the first few seconds following the frequency change [23].

1.1.3.3 Secondary Frequency Control

Secondary control typically replaces primary control after a matter of minutes and uses predetermined secondary reserve to bring the frequency back to normal levels [23]. This may be at the instruction of system operators. A common means of providing secondary frequency control is through Automatic Generation Control (AGC). This operates in conjunction with Supervisory Control and Data Acquisition (SCADA) systems, which gather frequency and generator output data from the system [24]. AGC software sends set-points to generators, which are automatically determined based on the energy balance in the area as well as considering the economical output [24].

In the National Electricity Market (NEM) in Australia, secondary frequency control services are provided by the Frequency Control Ancillary Services (FCAS) market, introduced in September 2001 [25]. Electricity providers bid in the market to provide frequency raise or lower services upon request. These include the fast raise and fast lower service, where a sudden frequency change is to be arrested within six seconds. Following this, slow raise and lower services stabilise the frequency within 60 seconds. Finally, the delayed raise and lower services bring the frequency back to normal operating levels [26].

1.2 Impact of Renewable Generation on Network Stability

Renewable generators generally tend to either have no rotational inertia, such as photovoltaic, or low inertia such as wind energy generators. In addition, many of these generators are connected to the grid via power electronic converters, essentially hiding any inertia that the generators may have. When these generators become a larger percentage of an electricity network, the decrease in inertia and frequency regulation capability of synchronous machines may lead to system instability or loss of synchronism when fault conditions occur [20]. These stability problems are an important issue that still needs to be addressed if the amount of non-synchronous generation in power networks is to be increased.

1.2.1 Stability Problems in a Network with Low Inertia

As a result of lower inertia, greater penetration of renewable energy generation has been shown to lead to problems in maintaining frequency. Research shows that increasing levels of doubly-fed induction generators (DFIGs) and greater amounts of high voltage DC interconnection alters the network frequency behaviour significantly [2]. As well as the deteriorating frequency stability with the high penetration of wind turbines, a significant reduction in damping capability is also observed due to the inability of DFIGs to provide damping support [6]. Rotor angle oscillations which occur are made worse when faults occur close to wind farms [6].

Loss of synchronisation is also a concern within weak grids. As rotors accelerate and decelerate according to the swing equation during disturbances, if the total inertia is small, the difference between acceleration and deceleration power may become large enough for the system to lose synchronisation [20]. Uncertainty in wind power output due to situations like gusts of winds, when wind penetration is high can also affect transient stability [3].

Reference [4] looks at the effect of increasing inverter penetration in a hybrid microgrid containing both a synchronous generator and an inverter (totalling 500 kVA) connected to the grid through an impedance. Results show that increasing the inverter penetration caused a reduction in stability.

1.2.2 Limits on Penetration of Renewables

Studies have also attempted to analyse the amount of wind penetration that could be added to a network before instability occurred. Reference [5] looks at limits to wind penetration, with limitations arising from system inertia and primary reserve requirements. The maximum admissible rate of change of frequency (ROCOF) is used as an equivalent to a minimum system inertia value. This is used to calculate the maximum wind power penetration in the Spanish power system. When wind power does not contribute to primary reserve or inertia, an inertia limit is reached between 79% (valley) and 66% (peak) penetration. To provide sufficient primary reserve, the limit is between 71% (valley) and 82% (peak) penetration.

Reference [7] also looks at the maximum penetration of DFIG based wind farms in a Chinese provincial power system. To preserve transient frequency stability, the maximum penetration is calculated to be 75% (for a 9 GW disturbance), although this number varies depending on the size of the disturbance. Stability is improved by adding spinning reserve and underfrequency load shedding.

1.3 Possible Solutions to Stability Problems

1.3.1 Inverter Control

While Reference [4] finds that increasing inverter penetration reduced stability in a hybrid microgrid, a number of ways to improve the stability are devised. Frequency and voltage control for the inverter, including $i_d - f$ and $i_q - V$ droops, helps to limit oscillations and reduce recovery time after islanding the microgrid. Another way that stability can be improved is by matching the inverter power factor to that of the local loads.

1.3.2 Virtual Inertia

In order to provide transient stability after events such as disturbances, the system needs to be able to provide a certain amount of power in the short term [18]. This has usually been provided by the rotating masses of synchronous generators. With fewer synchronous generators in the system, and more inverter interfaces, lower inertia could result in stability problems for the system.

In 2007, Reference [27] first proposed the idea that renewable electricity generators such as photovoltaic or solar could be made to appear as synchronous machines using a power electronics based approach . In this way, the properties of synchronous machines would continue to define the operation of the grid. Research into inverters that emulate the behaviour of synchronous machines, hence providing a source of virtual inertia, has continued [8–19]. Results based on simulations have shown that stability can be achieved with low or no mechanical inertia when inverters are equipped with virtual inertia [10].

The features that all virtual synchronous machine models have in common is that they all contain the mathematical model of a synchronous machine, with the inertia and damping characteristics being particularly important [15]. The virtual angular rotor position corresponds to the phase angle of the voltage induced by the virtual synchronous machine, while the voltage magnitude can come from either a synchronous machine electrical model or a separate reactive power control loop.

To most accurately represent a synchronous machine, including the transient and sub-transient dynamics, a full order model is needed. This is a seventh order model, including a fifth order electrical model and a second order mechanical model [27, 28]. Reference [15], however, argues that a full order model adds unnecessary complexity, as the most important proper-

ties, damping and inertia, are both already captured in the swing equation. Reduced order synchronous machine models are a commonly used alternative [11–14, 16]. In this case, the reactive power (and therefore voltage) is controlled separately, while the virtual synchronous machine handles the frequency and phase angle according to the swing equation.

Alternatively, inverters can contribute to grid inertia without using a synchronous machine model. This can done by tracking the grid frequency, as discussed in the European Union VSYNC project [8, 9]. However, a phase locked loop (PLL) is required for grid synchronisation, and therefore also external rotating inertia. This method is therefore not ideal for operation in weak grids.

Reference [15] also shows that droop control, used in converter dominated grids, can be equated to the reduced order synchronous machine model, with the droop gain and filter time constant directly related to the damping factor and the inertia constant in the swing equation of the virtual synchronous machine. This means that the parameters on a droop regulator can be tuned to emulate the behaviour of a synchronous machine.

Aside from the control systems, it also should be noted that fast short-term energy storage is required for the implementation of virtual inertia [18–20, 29]. According to the swing equation, energy needs to be absorbed or supplied in response to disturbances [20]. In the absence of kinetic energy stored in synchronous machines, alternative sources of energy storage are required in order to provide virtual inertia to the system. Energy storage devices are discussed in more detail in Section 1.3.3. The combination of a virtual synchronous generator with short term energy storage provides the ability to supply energy during disturbances and transients [29].

For modern variable speed wind turbines, such as full converter type turbines, rotor speed and frequency are not coupled. These wind farms therefore do not provide any inertia to the power system. With the addition of a control loop, variable speed wind turbines can imitate the inertial response of a synchronous generator and provide primary frequency control [6].

A common approach for providing inertia is to make use of the kinetic energy stored in wind turbine mass and blades [30–36]. Frequency control can be achieved by setting a non-optimal rotor speed or pitch angle, the downside being that wind generator will no longer be operating for optimal power transfer [31]. For DFIG wind turbines, for example, torque is applied to the rotor according to a predetermined curve, which is not based on the frequency of the power system and does not contribute any inertia [33]. A supplementary control loop is therefore needed to implement virtual inertia, adjusting the electrical torque set point in response to changes in grid frequency [31, 33]. For example, if the frequency decreases, the torque set point will increase, slowing the rotor and extracting kinetic energy [33]. Although using the turbine rotating masses to provide inertia has the advantage that no new parts are needed, its performance depends on the speed of the generator at the time of the disturbance, which is subject to the unpredictability of the wind speed [34].

It has also been found that while inertia-tuned wind farms improve the frequency response, oscillations occur which threaten the small signal stability [35]. A damping controller has been proposed to solve this problem, providing damping torque [35]. This was shown to help stabilise the system without affecting its frequency support ability.

Another means of providing the required energy is to use a super-capacitor across the DC link [34]. This has the advantage that its operation is independent of wind speed. Additional components will, however, be needed, as well as the re-rating of the grid-side converter [34].

1.3.3 Energy Storage

As mentioned earlier, the short term release of energy is required in response to disturbances. This is important for the stability of synchronous machines, as changes in power flow can cause synchronous machines to lose synchronisation [37]. However, kinetic energy such as that provided by synchronous machines can be compensated for using energy storage devices [20].

Energy storage can contribute to frequency stability, as they can be rapidly discharged following a disturbance [38]. Short-term energy storage can be connected to distributed generator buses to improve transient stability [29]. When considering the amount of energy required, References [20, 29] have also researched a method for estimating the sizing of energy storage devices to maintain system stability.

Another issue to consider is the availability of energy during low wind or low sunlight conditions. Energy storage technology will be able to allow the further increase of renewable generation within networks [37]. It is also able to decrease power fluctuations, such as those from sudden drops in wind power, this means that energy storage devices can help support grid frequency [37, 38]. Energy storage can also help to maintain adequate reactive power for voltage support [37].

Energy storage devices can be classified as mechanical (such as pumped hydro, compressed air or flywheels), electromagnetic (such as supercapacitors or magnetic energy storage), electrochemical (such as batteries), or thermal [37]. Flywheels and electromagnetic storage devices such as supercapacitors tend to operate on small time scales and are best for suppressing fast power fluctuations. A supercapacitor has already been installed in the Spanish isolated power system of La Palma for the purpose of frequency control [38].

1.4 Stability Issues in South Australia

The South Australian electricity network has one of the largest percentages of renewable energy in Australia. It is also relatively isolated, with the Heywood Interconnector being the only AC link to Victoria. From 2015 to 2016, rooftop solar generation was at 7.5% and wind generation was at 35% of the total electricity generated [39]. These numbers further increased

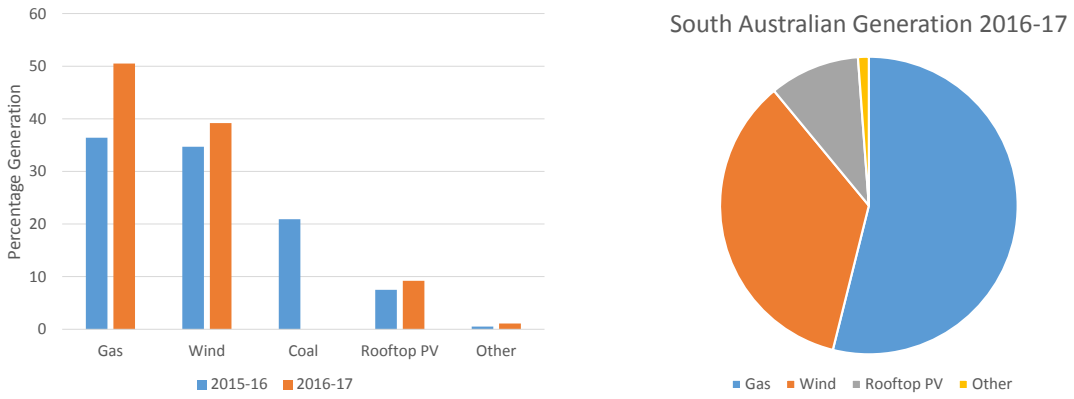

Figure 1.2 – South Australian generation mix [1, 39].

in 2016 to 2017, with rooftop solar at 9% and wind generation at 39% of the total generation within the state [1]. The generation mix in South Australia is shown in Figure 1.2. The drop in coal based generation seen in Figure 1.2 is due to the closure of South Australia's last coal-fired power station in Port Augusta in 2016. A single line diagram showing the South Australian transmission network, as well as the rest of Australia's NEM network, can be found on the Australian Energy Market Operator's (AEMO) website [40].

AEMO and Electranet have issued a report analysing the operation of the South Australian network when there is a low level of synchronous generation [41]. It was concluded that the network could operate reliably with a high percentage of wind and solar as long as the Heywood interconnector to Victoria is operational or as long as there is sufficient synchronous generation in South Australia. Unfortunately, this may not always be the case, as seen in the recent power outage that occurred in South Australia [42].

1.4.1 South Australian Blackout on the 28th of September 2016

A relatively recent example of stability problems occurring within South Australia was the blackout on the 28th of September 2016 [42]. Two tornadoes damaged two 275 kV transmission lines 170 km apart, causing the lines to trip. This resulted in a sequence of faults in quick succession over a two minute period. Due to protection settings on wind turbines, 456 MW of generation was tripped from several wind farms. This resulted in increased power flow from Victoria over the Heywood Interconnector. As the interconnector exceeded its capacity the lines were tripped, causing South Australia to become isolated from Victoria. As the amount of power being generated in South Australia was now much lower than the load, a collapse in frequency occurred resulting in the loss of all supply (or a Black System) lasting several hours.

1.4.2 Weakening of Primary Frequency Control

Another contributor to the stability problems in the South Australian Network could be the deterioration of the primary frequency control response under the FCAS market as discussed by Reference [43]. With the introduction of FCAS in 2001, mandatory governor response requirements have been removed, and governor deadbands were increased from 0.1 Hz to 0.3 Hz. The introduction of the "causer pays" penalties, in which market costs are allocated to generators as an incentive to better follow dispatch instructions, also penalises generators for providing good frequency response. This has led to a decline in the amount of primary frequency control being provided by generating units [43, 44].

With the FCAS market relying on secondary control, taking into account wider normal operating bands and measurement and communication delays from the SCADA network, the response to frequency deviations will be much slower. These delays mean that a larger amount of energy is needed to arrest a fall in system frequency and results in a greater chance of stability problems [43].

1.5 Research Aims

While power systems have largely consisted of synchronous generators for many years, renewable energy sources are becoming increasingly important. Synchronous generators are commonly being replaced by non-synchronous generating plants, such as solar or wind, often interfaced to the grid via inverters. With lower inertia from synchronous machines, this mixture of technology causes problems in power system stability.

The main aim of this research is to understand and investigate how a power system can be stable with large amounts of renewable generation, and subsequently, lower inertia from synchronous machines. As the South Australian electricity network currently has one of the largest percentages of renewable generation in Australia, and is relatively isolated with the Heywood Interconnector being the only AC link connecting it to the eastern states, a simplified network model of the South Australian network will be developed in PSCAD as a case study.

Using this representation of South Australia developed in PSCAD, simulations will be run to determine what levels of inverter penetration the network can handle before it becomes unstable in response to faults. The effect of inverter controls on the stability of the network will also be investigated.

In addition to fault simulations, the network stability will also be tested against tripping one or both of the two parallel interconnector lines, the second case testing the isolation of the South Australian network. Different levels of power transfer across the link will be tested, with the aim of determining the amount of synchronous generation that is required for stability in each case. Work will be done in an attempt to improve the stability of the network and allow for greater inverter based generation by improving the inverter controls.

To summarise, the main aims of this research are to:

- Develop a simplified network model of the South Australian network in PSCAD
- Determine the level of inverter penetration that the network can handle before it becomes unstable in response to network disturbances
- Investigate the effect of inverter control on the stability of the network
- Attempt to improve the stability of the network to allow for greater levels of inverter penetration

1.6 Thesis Outline

This thesis is organised as follows: Chapter 2 discusses the design of the network in PSCAD which will be used in this research. It discusses how a model of the South Australian electricity network, along with its connection to Victoria through the Heywood Interconnector, is designed for use in PSCAD simulations. It is represented as a simplified network with a synchronous generator and inverter representing the aggregated synchronous and non-synchronous generation within the state.

Initial simulations performed using this PSCAD model of the South Australian network are discussed in Chapter 3. The stability of the network is analysed in response to network disturbances. The effect of inverter penetration is assessed by increasing the size of the inverter while decreasing the size of the synchronous generator in the PSCAD representation of the South Australian network. Based on these results, improvements to the network are also made. Improvements to the design of the inverter controls and how they are tuned using the loop shaping technique is also discussed.

After these improvements are made to the network, Chapter 4 will analyse the stability of the network at different inverter penetration levels in response to various faults applied to the network. This chapter then considers the effect of inverter penetration in the event of the disconnection of the Heywood Interconnector and the islanding of the South Australian Network. Finally, Chapter 5 presents the conclusions and provides recommendations for future work.

2 Network Design

2.1 Introduction

Renewable generators, which are often asynchronous, are becoming a larger part of electricity networks around the world. This has led to concerns about the stability of networks where the proportion of synchronous generation is decreasing. To investigate the effect of inverter penetration on stability of a network with mixed synchronous and asynchronous generation, a simplified network model of the South Australian network has been developed in PSCAD as a case study.

The South Australian electricity network has been chosen as a case study because it currently has one of the largest percentages of renewable energy in Australia. Within South Australia, rooftop solar generation was at 9% and wind generation was at 39% of the total electricity generated from 2016 to 2017 [1]. The network is also relatively isolated, with the Heywood Interconnector being the only AC link to Victoria and the rest of eastern Australia.

To form the simplified network model, aggregate generator models are used to represent the power generated in South Australia from either synchronous generators or inverters. Loads are also represented as aggregate models and are separated intro three main types: constant impedance, constant power and motor based loads. The Heywood Interconnector is represented by two parallel lines connecting to an external system. This external system, representing the eastern states in the NEM, is modelled as a large synchronous generator and load.

The network designed in this chapter will be used to analyse the stability of a network when the ratio of inverter based generation to synchronous machine based generation is increased. The effect of different types of inverter control will also be considered. This chapter discusses the different components of this network in detail.

2.2 Software

Before work could begin, appropriate software needs to be selected for simulating the power system. The chosen software needs to be able to handle transient dynamics, as this research involves analysing the transient stability of networks.

PSCAD is a commonly used professional tool for the simulation and analysis of power systems [45]. This software has been chosen due to its particular focus on the dynamics within equipment, such as within generators, rather than focusing mainly on the network dynamics as many other power system software tends to do. For this reason, PSCAD has been chosen for use in these studies.

2.3 Network Layout

A network model has been created in PSCAD to represent the South Australian electricity network and its connection through to eastern Australia via the Heywood Interconnector. The network has been simplified for ease of simulation, with a single synchronous generator representing the total synchronous generation in South Australia. All energy generated through the use of inverters, such as wind and solar for example, is represented through a single inverter.

The network design is shown in Figure 2.1. The South Australian side is represented as having 2000 MW of generation, which can be composed of varying proportions of synchronous and asynchronous generation. A 2000 MW rated synchronous generator represents the synchronous generation in SA, which is able to be displaced by an X MW inverter.

The loads in the South Australian network are represented as being equally divided between constant impedance, constant power (with reactive power proportional to V^2), and induction motor loads with inertia. The impedance (Z) in Figure 2.1 represents the AC link between South Australia and Victoria, the Heywood Interconnector. The power consumed by the loads can be varied to change the amount of power flow across the Heywood Interconnector. In Figure 2.1, the load in South Australia is set to 1500 MW in total, with the three types of load each consuming 500 MW. As the power generated in South Australia is 2000 MW, this results in 500 MW of power being transferred through the link into Victoria. The external system, representing eastern Australia, is represented as a 20,000 MW synchronous generator and a load of approximately 20,000 MW.

The system frequency is set to 50 Hz, the nominal frequency in Australia. Nominal voltages within the network are 275 kV RMS line to line in the South Australian side of the network and 500 kV RMS line to line in the external system.

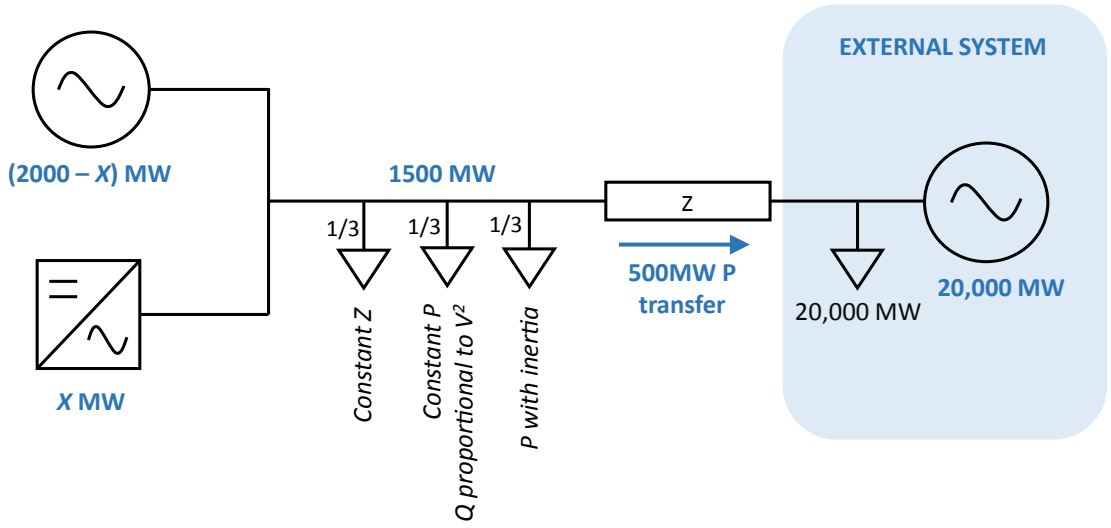

Figure 2.1 – PSCAD network diagram.

2.4 Synchronous Machines

To represent the power produced from synchronous generators, a 2000 MW rated salient-pole synchronous generator is used for the South Australian system, with a similar 20,000 MW machine being used for the external system. The field voltage is controlled by a standard IEEE type STA1 exciter, and a PSS1A power system stabiliser (PSS) is also being used to help damp oscillations. The exciter and stabiliser are available in the PSCAD component library; details can be found in Reference [46]. The parameters used in the exciter are obtained from Reference [21]. The PSS parameters use the default provided with the PSCAD PSS1A component. The generator, exciter and PSS parameters are included in the Section A.1 of the Appendix.

For the larger 20,000 MW generator, mechanical torque is controlled by a hydro turbine and governor. For this, the IEEE GOV3 governor model, which is available as a component in PSCAD, was used. This governor outputs the gate position into the hydro turbine to control its speed, which then outputs mechanical torque to the synchronous machine. The smaller 2000 MW generator is not controlled by a governor, but rather is set at fixed power. This is done by inputting a constant level of torque into the 2000 MW generator on the South Australian side of the system.

The reason for not having governors on both of the synchronous generators is due to the fact that the governor models available in PSCAD are not able to properly keep the machines at a set power value. For example, the synchronous generator in South Australia is not able to be kept at 1500 MW when the inverter power is 500 MW. This also affects the ability to control the power flow across the interconnecter. Due to this problem a governor is only kept on one of the generators. The governor is added to the larger 20,000 MW machine rather than the smaller 2000 MW generator because if the governor is present on the smaller machine only, the

machine is not of a large enough size to adequately control the network frequency. It should be noted that a governor and turbine has later been designed for the 2000 MW generator in the South Australian system representation. Details of these network improvements, which are applied to later simulations, are discussed in Chapter 3.

The generators are also connected to the grid by 16/275 kV delta-wye transformers, with losses of 0.06 PU. Transformer tap positions are also adjusted to help keep the voltage at the required level (275 kV for the South Australian network and 500 kV for Victorian side).

2.5 Loads

To represent the loads in the South Australian network, three separate types of loads are used. This allows representation of the different types of load that are typically present in the power system. The amount of power consumed by the load is equally divided amongst the three types: constant power, constant impedance, and an induction machine load. The larger 20,000 MW in the external system is a constant power load. For initial simulations, the load in South Australia is set at 1500 MW, allowing a flow of 500MW across the Heywood Interconnector.

Loads are modelled in PSCAD according to the relationship

$$P = P_o \cdot (\frac{V}{V_o})^{NP} \cdot (1 + K_{PF} \cdot dF) \qquad Q = Q_o \cdot (\frac{V}{V_o})^{NQ} \cdot (1 + K_{QF} \cdot dF) \tag{2.1}$$

where P and Q are the load real and reactive power, P_o and Q_o are the rated real and reactive power, V is the load voltage, V_o is the rated load voltage, NP is the dP/dV voltage index for real power, NQ is the dP/dV voltage index for reactive power, K_{PF} is the dQ/dF frequency index for real power, and K_{QF} is the dP/dF frequency index for reactive power.

The first 500 MW load is constant impedance, with power being proportional to the square of the voltage. Both NP and NQ are set to two in the PSCAD load model to give constant impedance. The second load is constant power, but with reactive power being kept at constant impedance, with reactive power proportional to the voltage squared. In this case, NP is set to zero and NQ is set to two. In both the constant impedance and constant power loads, K_{PF} and K_{QF} are set to zero. In both these cases, the reactive power level is set to zero for initial simulations. The final 500 MW is a machine based load with inertia, which is represented by a wound rotor induction machine representing the combined motor loads. The parameters for this machine are included in Table A.4 in the the Appendix.

In later simulations, after Chapter 3, the proportions of these loads are altered by halving the induction motor load, making it one sixth of the total load, or 250 MW. This is to make the proportion of machine loads closer to what is realistically seen in a network. The remaining two loads are divided evenly between the remaining 1250 MW load power, 625 MW each.

Table 2.1 – Impedances separating SA and VIC.

Victoria - South Australia Interconnection			
All impedances on 100MVA base			
From	**To**	**R**	**X**
		pu	**pu**
500 kV Lines (2 lines)			
Melbourne	Moorabool	0.00045	0.006747
Moorabool	Tarrone	0.000154	0.02041
Tarrone	Heywood	0.00413	0.00549
Total 500kV Lines		0.004734	0.032647
275 kV Lines (2 lines)			
Heywood	South East	0.0071	0.049
South East	Tailem Bend	0.0229	0.167
Tailem Bend	Adelaice	0.0046	0.0345
Total 275 kV		0.0346	0.2505
500/275 kV transformer	**(2 transformers)**		
		0.003	0.02
Total 1 500 kV line, 1 transformer, 1 275 kV line			
		0.042334	0.303147
	Rounded	0.04	0.3

2.6 Interconnector

Two parallel lines with impedances represent the Heywood Interconnector, which connects South Australia to Victoria. The link is represented as two 275 kV lines from Adelaide to Heywood and two 500 kV lines from Heywood to Melbourne separated by two 275/500 kV transformers. Impedances are estimated according to Table 2.1, courtesy of Professor Peter Wallace. Inductances on the 275 kV lines have been lowered to 0.01 H to improve stability. This adjustment can be explainable due to the presence of series capacitors in the network.

2.7 Inverter

A representation of the inverter and its control is shown in Figure 2.2. The inverter model is made up of six IGBT switches, the switching pulses being generated from a Hysteresis Current Control PWM Generator. The inverter is connected to the grid through an LCL filter and a delta-wye transformer. The inverter is powered by a DC voltage source of 1200 kV. A phase locked loop (PLL) component from PSCAD is used to track the phase of the three phase voltage.

The proportional gain used in the PLL is 50 and the integral gain is 900.

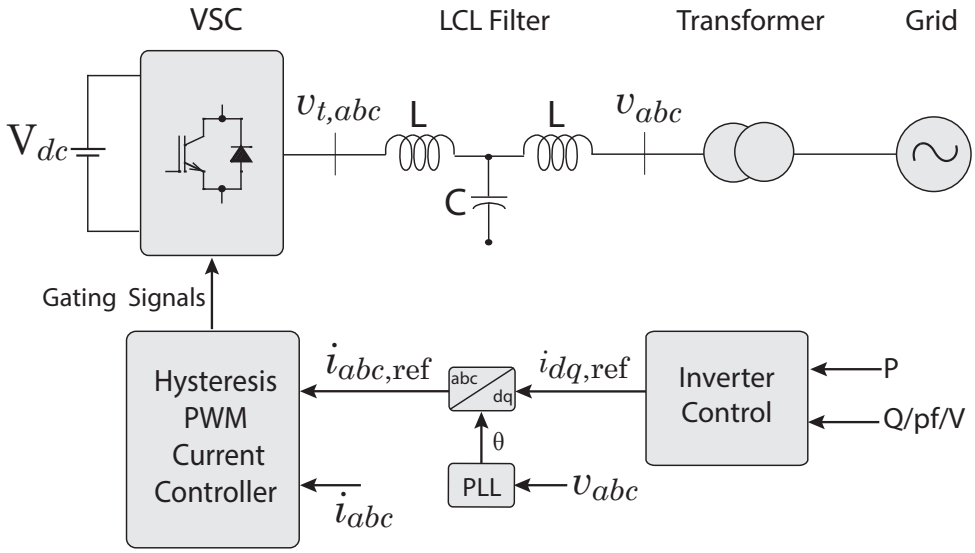

Figure 2.2 – Inverter design.

Sections 2.7.1 to 2.7.3 describe the inverter control design, represented by the "Inverter Control" block in Figure 2.2. For initial simulations in Chapter 3, three types of inverter control are compared. The first is an algebraic control with fixed real and reactive power. The second is PI control with real and reactive power control, which can be altered for power factor control if desired. The third is PI control with power and voltage control. The following subsections discuss these control systems in more detail.

As seen in Figure 2.2, the inverter control block is designed to control the active power and reactive power (or alternatively power factor or voltage). It produces the d and q current reference signals for the inverter. The current reference is converted back to the abc reference frame by a dq to abc conversion block, with the angle of transformation obtained from the PLL. The three phase reference current is then input into the current controller where it is compared with the measured three phase current. The hysteresis current control PWM generator then generates the gating signals that control the inverter.

As the PI controllers for the inverter control have been tuned using a trial and error method, this leaves a lot of room for improvement. These improvements are discussed in more detail in Chapter 3. Another thing to note with the inverter is that the large voltage source assumes that energy is readily available when controlling power, at least for the short term. This could be from energy storage devices, such batteries for example, or perhaps by running wind turbines below maximum power levels. The ability to absorb or supply reactive power is also assumed.

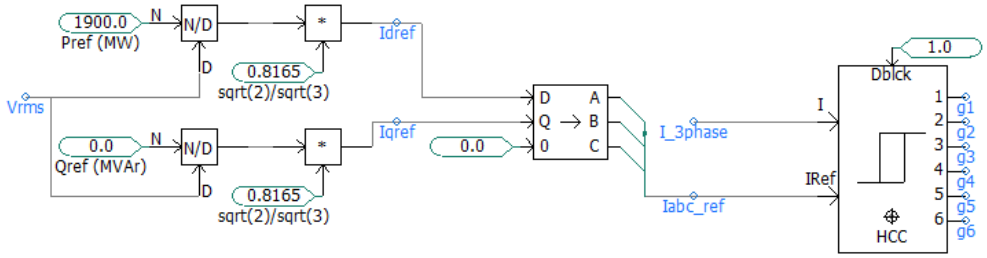

Figure 2.3 – Algebraic inverter control.

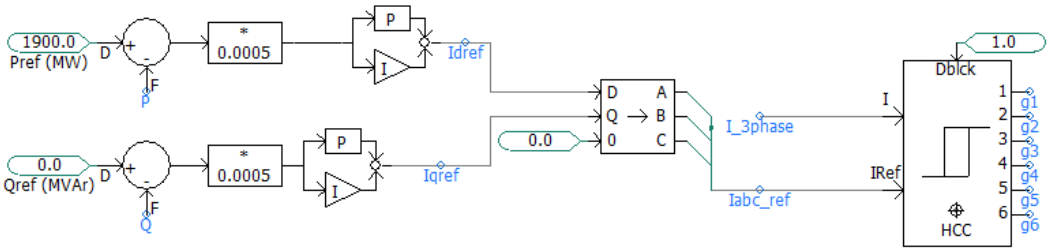

Figure 2.4 – PI control of active and reactive power.

2.7.1 Algebraic Control

For the algebraic control, the direct and quadrature axis reference currents, i_d and i_q, were simply calculated by dividing the reference power by the voltage as shown in Figure 2.3. The dq reference currents are converted into the three phase reference currents via a dq to abc transform block, with the angle of transformation determined by a phase locked loop. The current reference is then compared with the measured three phase current within a hysteresis current control PWM generator (or HCC), which generates the IGBT switching pulses (g1 to g6) that control the IGBT switches of the inverter.

2.7.2 PI Control of Active and Reactive Power

A PI control scheme has also been designed to control the active and reactive power of the inverter as shown in Figure 2.4. Measured real and reactive power are subtracted from their reference values and converted into PU values before being input into PI controllers. The PI controllers used proportional gains of one and integral time constants of 0.01 seconds. The PI controllers then give the d and q current reference values, which are again input into the hysteresis current control block after being converted into the abc reference frame. This control scheme could be adjusted to give power factor control, as shown in Figure 2.5. Here a power factor reference was converted into the phase angle θ. As $tan(\theta)$ is equal to the reactive power divided by the active power, $tan(\theta)$ is multiplied by the active power to give a reactive power reference value. This reactive power reference was then compared with the measured value and input into a PI controller as described above.

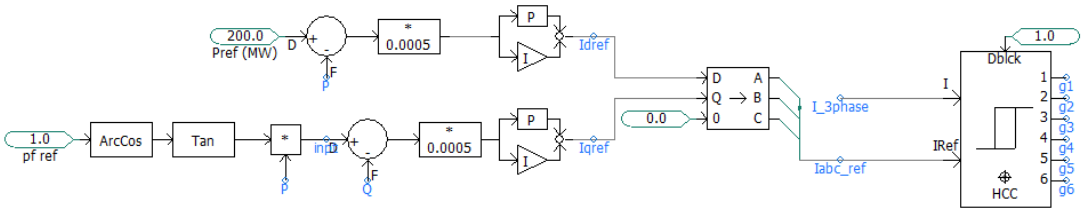

Figure 2.5 – PI control of power and power factor.

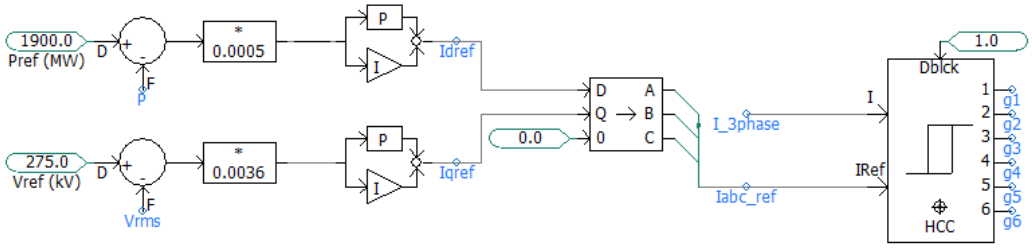

Figure 2.6 – PI control or power and voltage.

2.7.3 PI Control of Active Power and Voltage

The inverter PI controllers can also be used to give voltage control, as shown in Figure 2.6. It is common in power networks for voltage to be controlled using reactive power. While the power control is still the same in Section 2.7.2, the reactive power control has been replaced with voltage control. The RMS line to line voltage is subtracted from a reference value and, after being converted to PU, is input into a PI controller to give the i_q reference current. The proportional and integral gains of the PI controller remain the same.

2.8 Limitations

It should be noted that results may not accurately represent the South Australian network due to the simplified nature of the aggregate models of the synchronous generators and inverters. However this is still a good starting point to look at this problem of mixed networks of inverters and synchronous generators.

As there is only a governor present on the larger 20,000 MW synchronous generator, as explained in section 2.4, improvements will also need to be made to the governors to make the simulations more realistic with governors present on both synchronous generators. This is discussed in Section 3.4, where a governor is designed for the 2000 MW synchronous generator. The PI controls of the inverter have so far only been turned using a trial and error method, which means that the inverter controls are not as good as they could be. An attempt to make the inverter model more realistic and to improve the tuning of the inverter is discussed in Section 3.3.

2.9 Conclusions

A simplified representation of the South Australian electricity network in PSCAD is discussed in this chapter. The network has been designed in order to study the effect on inverter penetration on the stability of a network.

The network is represented with a synchronous generator and inverter representing the aggregated synchronous and asynchronous generation within South Australia. The Heywood Interconnector is also included so that the power flow between South Australia and Victoria can be modelled. A large generator and load is used on the other side of the link to represent the electricity generated in eastern Australia. Loads in South Australia are modelled as a mixture of constant power, constant impedance, and induction motor loads. Several types of inverter control systems have also been designed. These include algebraic control, PI control of active and reactive power, as well as PI control of active power and voltage.

Next, in Chapter 3, simulation based studies are carried out using the PSCAD network designed in this chapter. The proportion of power generated by the aggregate synchronous generator and inverter models will be varied in order to investigate the effect on network stability. The effect of different types of inverter control will also be considered. As this PSCAD based network design does still have a number of limitations, the network designed in this chapter will also be improved upon in an attempt to improve stability. In particular, improvements will be made to the design of the inverter controls and governor control will be added to the South Australian synchronous generator representation.

3 Initial Simulations and Network Improvements

3.1 Introduction

A simplified model of the South Australian electricity network, along with its connection to Victoria through the Heywood Interconnector, has been designed in PSCAD. The details of how this network is designed are discussed in Chapter 2. The PSCAD network models the combined amounts of synchronous and inverter-based generation within the South Australian network, where the proportions of synchronous and asynchronous generation can be altered. The aim is to test the stability of the network in response to disturbances as the proportion of asynchronous generation increases within the network. The effect of inverter control on stability is also considered.

To test the stability of the network, a single phase fault is applied to the South Australian network representation. A number of simulations are run, described in Section 3.2. Each time, the power produced by the inverter, representing the asynchronous generation within South Australia, is increased. At the same time, the power produced from synchronous generation is decreased, keeping the overall amount of power generated within South Australia constant. For each inverter power level that is tested, three different types of inverter control are tested. These inverter control systems are algebraic control, PI control of real and reactive power, and PI control of power and voltage. These control systems are described in more detail in Chapter 2, Section 2.7.

Based on these initial simulations, several improvements need to be made to the network to improve the accuracy of the results. To begin with, improvements are made to the design of the inverter. Section 3.3 discusses changes made to the inverter to make it more realistic. As the PI controllers for the inverter have so far only been tuned by using a trial and error method, the inverter PI controls for active and reactive power are now tuned using the loop-shaping method. Improvements are also made to the inverter current controller. Further simulations are then run to see if improvements have been made to the network stability.

As mentioned in Chapter 2, there is no governor present on the synchronous generator model in the South Australian network representation. As none of the governor models within PSCAD have the capability to keep a generator at a set power, a suitable governor is designed for use with this generator as discussed in Section 3.4. Finally, Section 3.5 discusses changes made to the modelling of the loads in the South Australian network representation.

3.2 Fault Simulations

As inverter-based generation increases within a network, it is possible that the transient stability of the network may be negatively affected. To test whether this is the case, faults are applied to the South Australian network representation in PSCAD in order to test the stability of the network at different inverter penetrations. As well as looking at different levels of inverter penetration in the network, three different types of inverter control are also used to see which one better controls the inverter as inverter penetration increases.

For the network to remain stable after the fault, it is expected that synchronous generators remain synchronised and return to a steady state condition after the fault is cleared. Oscillations must also be damped. This satisfies the rotor angle stability requirements described in Section 1.1.1. Voltage and frequency stability also need to be met. Network voltages need to be returned to the normal range of 0.9 to 1.1 PU after the disturbance [47]. The frequency operating standards for the mainland require that frequency is contained within 49 to 51 Hz, then stabilised between 49.5 to 50.5 Hz within one minute, then returned back to the normal operating band (49.85 to 50.15 Hz) within five minutes [48].

The fault is applied as a single phase to ground fault for 100 ms seconds, after which the lines are restored. Firstly, faults are applied at different locations in the network to find the worst case scenario in terms of network stability. This happens to be at the 275 kV bus at the connection point for the inverter and loads on the South Australian side of the network. This fault location is chosen for all further simulations. The fault impedance to ground is 0.01 Ω.

Fault simulations are run with varying levels of inverter power (X) using the three inverter control schemes described in Section 2.7. Synchronous generator power is set at 2000 - X MW. Simulations are run and the network is allowed to reach steady state, leaving time for the synchronous machines and other components to initialise. The fault is then introduced after 80 seconds, after which the simulation is run for a further 40 seconds, 120 seconds in total.

Figures 3.1 to 3.3 show the network response after the fault for inverter powers of 500, 1000, and 1500 MW. The remaining power produced from the synchronous generators is therefore 1500, 1000, and 500 MW. Three different types of inverter control are compared. The first is algebraic control with fixed real and reactive power. The second is PI control of real and reactive power, and the third is PI control of power and voltage.

RMS line to line voltage, synchronous generator power, frequency, voltage phase angle, inverter power, and inverter reactive power are measured from just before the occurrence of the fault at 80 s until 100 s. The voltage is measured on the 275 kV line on the South Australian side of the Heywood Interconnector. The frequency and phase angle are measured near the South Australian aggregate synchronous generator.

Looking at the effect of inverter controls in Figures 3.1 to 3.3, the response of the RMS voltage to the fault is generally similar for algebraic control and PI (P and Q) control, however, the response is worse when using PI (P and V) control. This is also true of the inverter real and reactive power, which also shows the worst response with voltage control, with high amounts of reactive power being drawn to help control the voltage. The best response seen in the inverter real and reactive power tended to be from the PI active and reactive power control. The frequency response also appears worse when using PI voltage control . This is also true for the synchronous generator power, especially at 500 MW inverter power. The PI control of inverter real and reactive power does not appear much different from the algebraic control.

To get a better comparison of different levels of inverter penetration (X), the three different levels of inverter power are compared side by side in Figure 3.4. The inverter is in this case controlled using PI control of active and reactive power. Looking at the synchronous generator power, the response after the fault occurs is improved at 1000 MW inverter power (synchronous generator at 1000 MW) compared to 500 MW inverter power (synchronous generator at 1500 MW). The response of the synchronous generator then becomes worse at 1500 MW inverter power (synchronous generator at 1000 MW). The same is true for the frequency (and phase angle), with the 1000 MW inverter case giving the best response, followed by the 500 MW inverter then the 1500 MW inverter. When looking at RMS voltage, it can clearly be seen to worsen as inverter penetration increases. This is also true for inverter power. Inverter reactive power also gives the worst response at 1500 MW inverter power, with the best response being at the inverter power of 1000 MW.

3.2.1 Discussion of Results

As discussed earlier, both the synchronous generator power and frequency responses to the single phase fault improved with inverter penetration, at least up to about 1000 MW. It also appears that the synchronous generator power response has better damping. This however could be due to the smaller size of the synchronous generator as inverter power increases. At higher levels of inverter penetration, however, the responses begin to deteriorate. It should be noted that there is no governor present on the South Australian synchronous generator, so these responses may improve if a governor is present.

As inverter power increases, network responses to faults are generally less stable. Larger peaks are observed in the RMS voltage and there is more noticeable oscillation as inverter power increases, although the oscillation is likely from the inverter switching. The responses seen in the inverter active and reactive power are also worse at higher inverter powers.

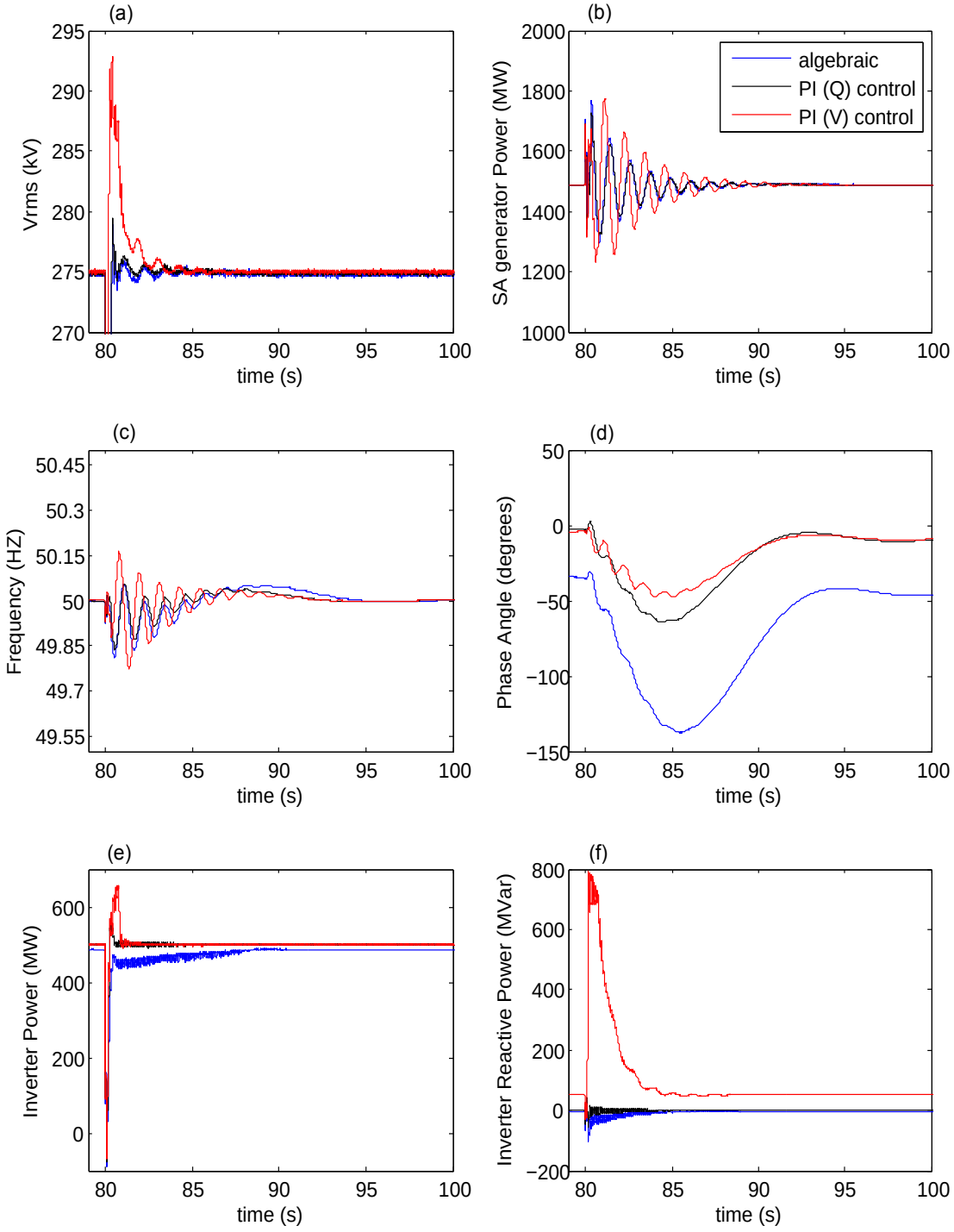

Figure 3.1 – Response after 100ms single phase to ground fault in a network with a 500 MW inverter using algebraic control (blue), P and Q PI control (black), and P and V PI control (red) showing (a) RMS line to line voltage (b) synchronous generator power (c) frequency (d) voltage phase angle (e) inverter power and (f) inverter reactive power.

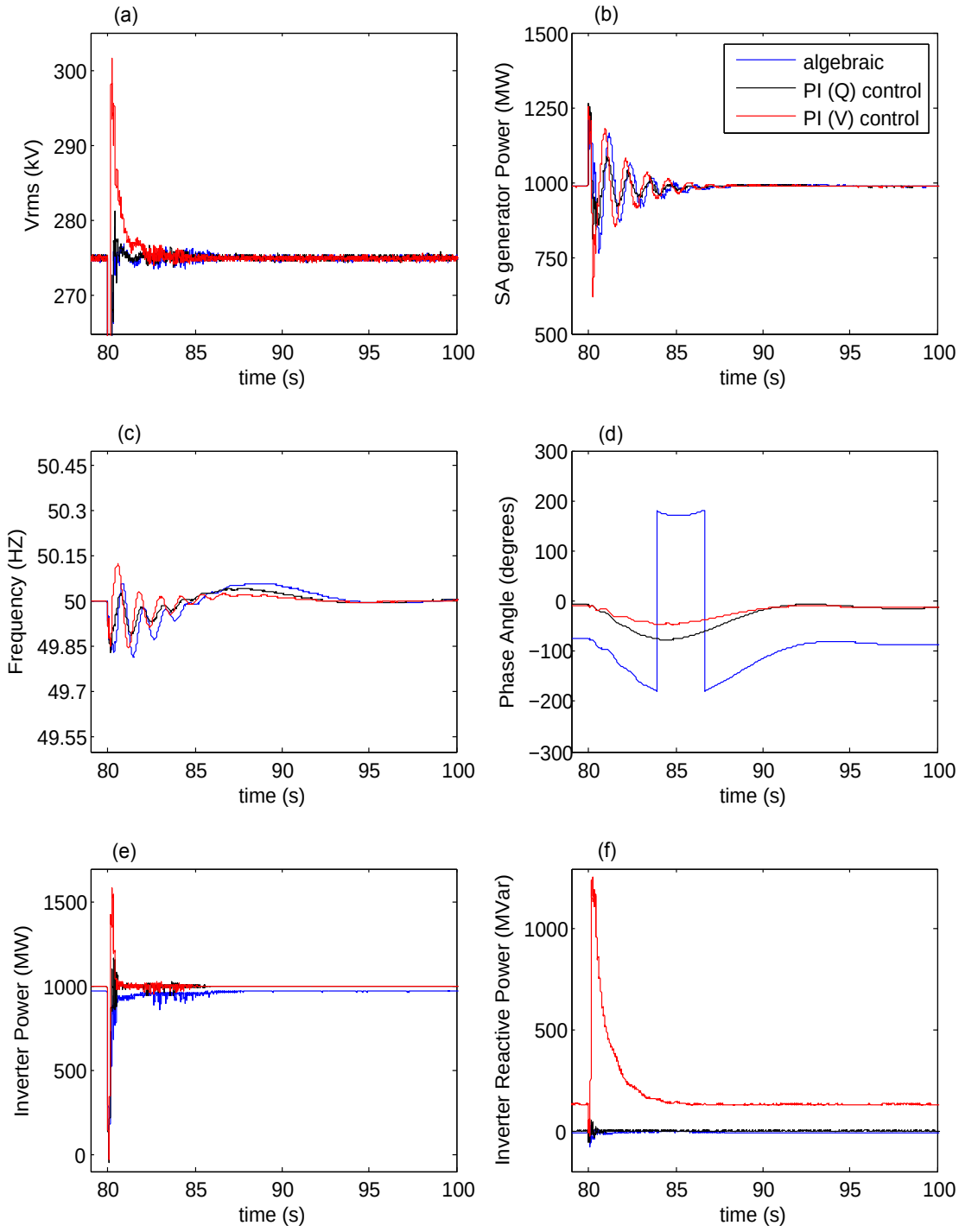

Figure 3.2 – Response after 100ms single phase to ground fault in a network with a 1000 MW inverter using algebraic control (blue), P and Q PI control (black), and P and V PI control (red) showing (a) RMS line to line voltage (b) synchronous generator power (c) frequency (d) voltage phase angle (e) inverter power and (f) inverter reactive power.

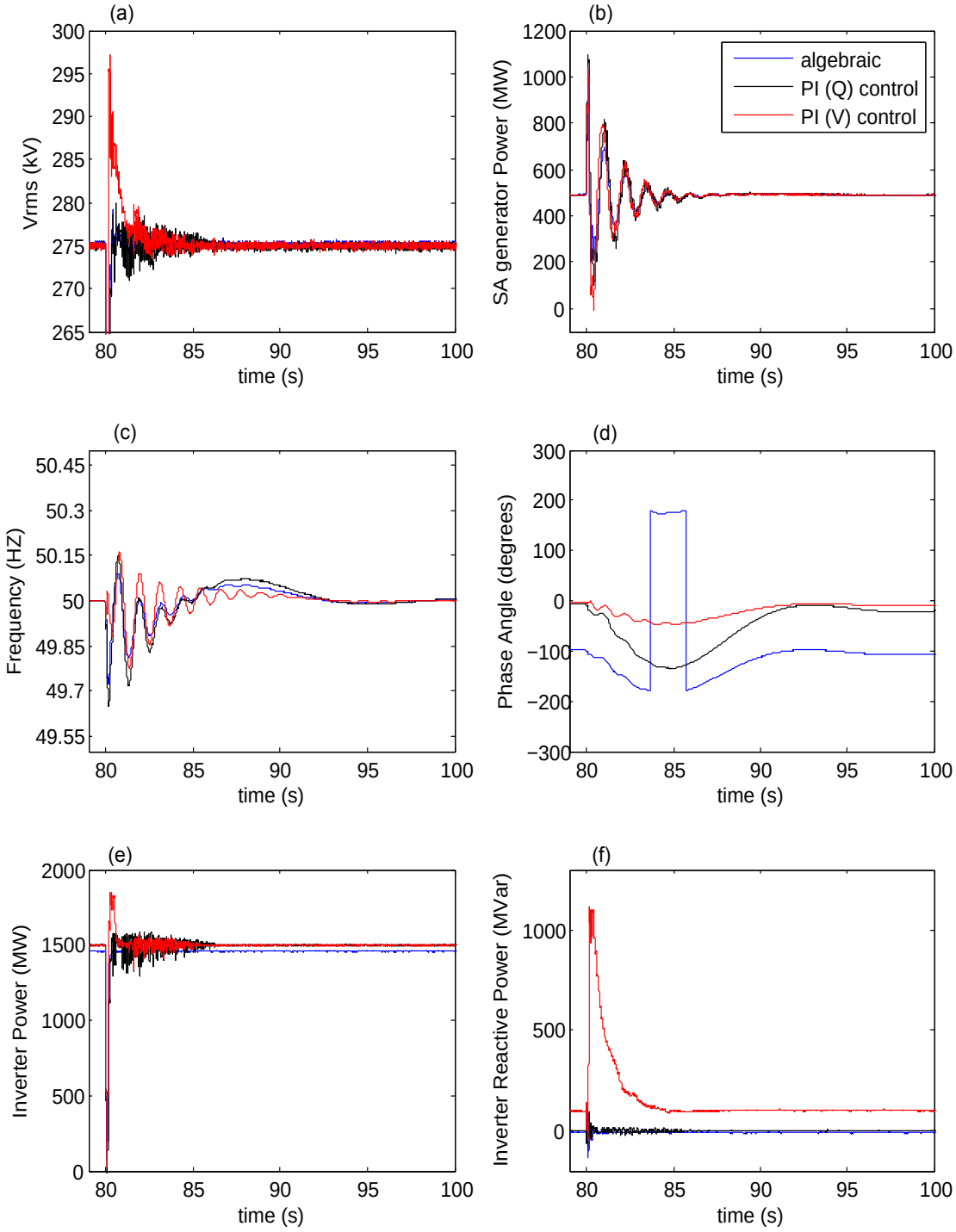

Figure 3.3 – Response after 100ms single phase to ground fault in a network with a 1500 MW inverter using algebraic control (blue), P and Q PI control (black), and P and V PI control (red) showing (a) RMS line to line voltage (b) synchronous generator power (c) frequency (d) voltage phase angle (e) inverter power and (f) inverter reactive power.

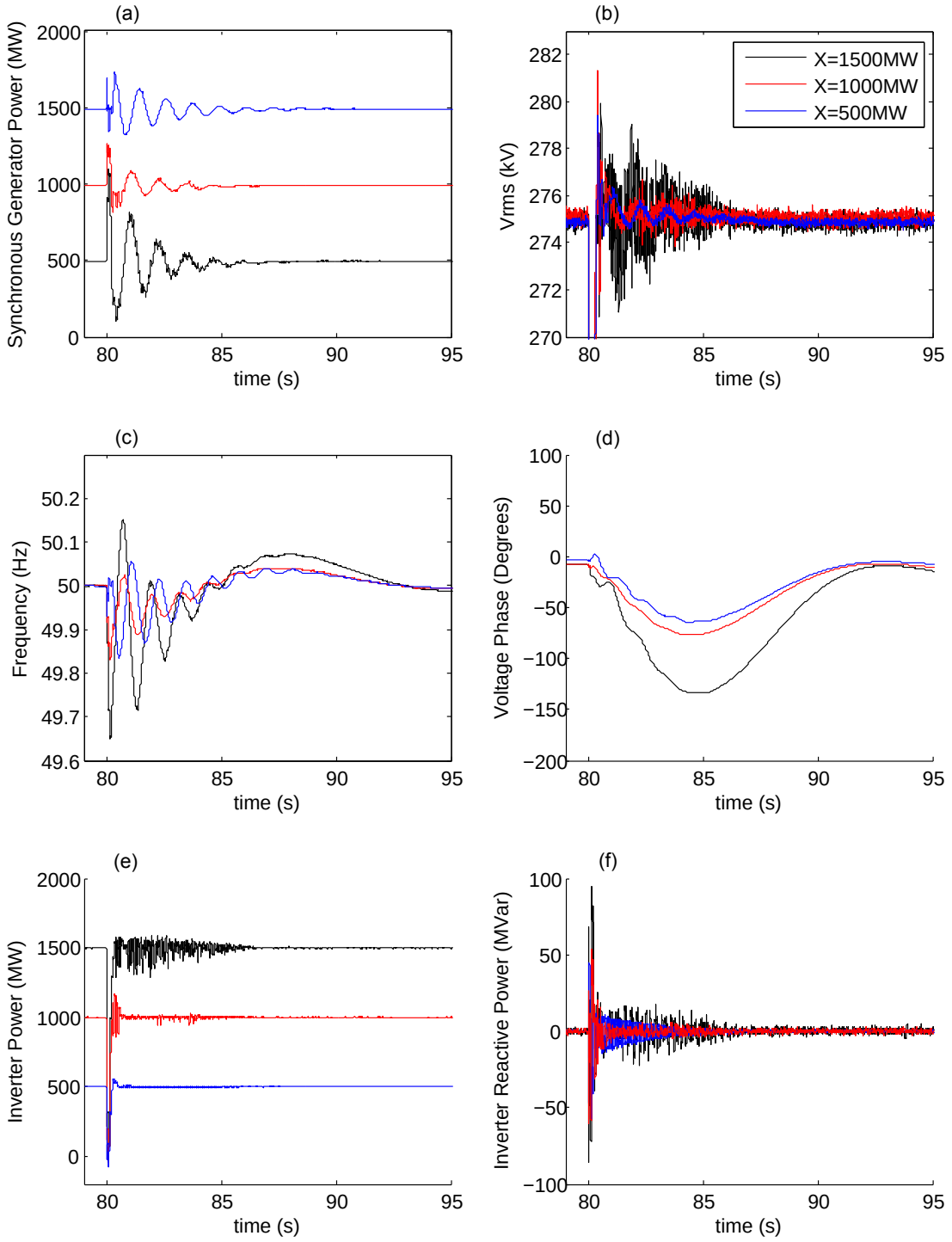

Figure 3.4 – Response after 100ms single phase to ground fault in a network with a 500 MW inverter (blue), 1000 MW inverter (red), and a 1500 MW inverter (black) using P and Q PI control showing (a) synchronous generator power (b) RMS line to line voltage (c) frequency (d) voltage phase angle (e) inverter power and (f) inverter reactive power.

Looking at the effect of inverter controls, the PI control of active power and voltage tend to be less effective than both algebraic control and PI real and reactive power control. PI real and reactive power control is perhaps only slightly better than the algebraic control, although not by much.

These responses show that there may be a problem with the inverter controls. The PI voltage control draws large amounts of reactive power, while the inverter active power also shows large spikes and a lot of noise. As the PI controls for the inverters are tuned using a trial and error method, this is likely the cause for much of the poor inverter behaviour. The next step in ensuring accurate results is to make sure to properly tune the inverter controls. Before accurate conclusions can be drawn, improvements need to be made to the inverter. A governor will also need to be added to the South Australian synchronous generator to give more realistic results.

3.3 Improvements to Inverter Design

As discussed above, the response of the inverter to disturbances can be improved. This section discusses changes that are made to the inverter. Firstly, in Subsection 3.3.1, inverter voltages are altered to more realistic values. Next, the hysteresis current control PWM generator is replaced with a more conventional dq current controller (Subsection 3.3.2) and a PWM generator is designed (Subsection 3.3.3). The inverter active and reactive power PI controls are then tuned using loop-shaping, as described in Subsection 3.3.4. Finally, in Subsection 3.3.5, these inverter improvements are tested in response to a fault.

The new inverter design is shown in Figure 3.5. The PI controllers control the inverter real and reactive power and generate the d and q axis reference currents which are input into the dq current controller. This then sends out dq axis voltage control signals which are input into a PWM generator after being transformed into the abc reference frame. The PWM generator then produces the gating signals controlling the inverter.

3.3.1 Inverter Voltages

To begin with, changes are made to the inverter voltages to make it more realistic. Inverter voltages are altered to more realistic values, such as those likely to be used in wind generators. The AC voltage at the inverter terminal is changed to 690V line-line and the DC voltage is set to 1.2 kV. However, it should be noted that the DC voltage did need to be increased later so that the inverter could generate enough current for the power required.

3.3.2 Current Control

The inverter control used in the initial simulations in Section 3.2 contains an outer control loop, controlling active and reactive power for example, as well as an inner current control loop.

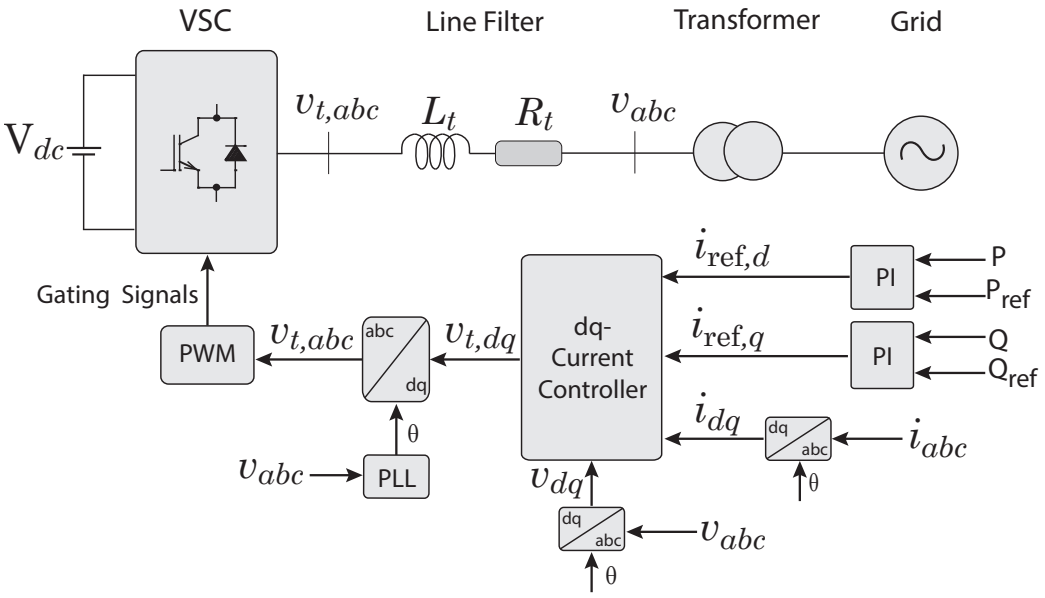

Figure 3.5 – Improved inverter design.

The outer control loop generates the i_d and i_q reference currents needed for the inverter to output a given amount of active and reactive power. The inner current control loop generates the voltage control signals used in the PWM generator to generate the inverter IGBT switching signals. Initially, the inner current control is performed by the hysteresis current control PWM generator (or HCC) component that is available in PSCAD. As well as current control, this component also includes a PWM generator to which outputs switching pulses to the inverter. The pulses generated keep the measured currents within a defined band around the reference current.

In an attempt to improve the behaviour of the inverter, the hysteresis current control is replaced with a more conventional PI based current controller. This design of this dq current controller is shown in Figure 3.6. The d and q axis are used as they are almost fully decoupled, allowing control of one axis without affecting the other. This allows for separate control of real and reactive power. $i_{t,d}$ and $i_{t,q}$ are the d and q currents at the inverter terminal, while $i_{\mathrm{ref},d}$ and $i_{\mathrm{ref},q}$ are the reference currents. v_d and v_q are the d and q axis inverter terminal voltages, and $v_{t,d}$ and $v_{t,q}$ are the voltage control signals sent into the PWM generator. ω is the angular velocity and L_t is the filter inductance at the inverter output.

As seen in Figure 3.6, the d and q current errors (reference current minus measured current) are fed into PI controllers. The signals are then added to the inverter terminal voltages v_d and v_q as well as the decoupling components, ωL_t. $v_{t,d}$ and $v_{t,q}$ are then sent to a PWM generator.

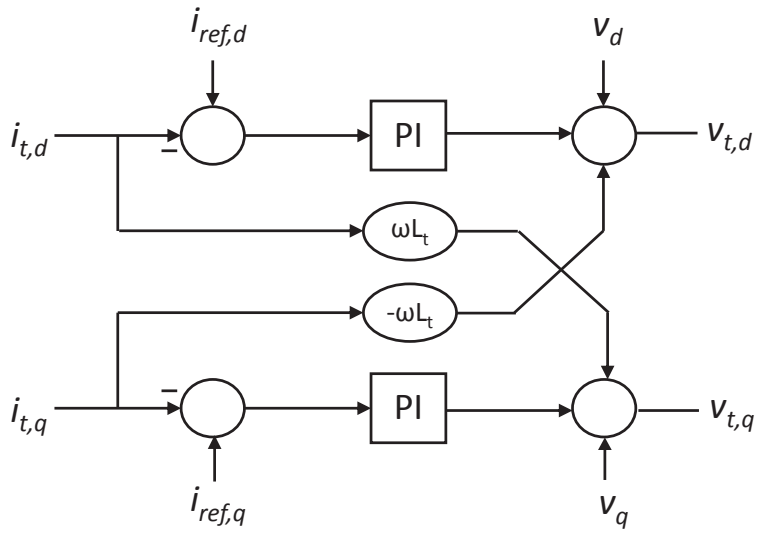

Figure 3.6 – Standard inverter dq current control.

The PI controller is designed following the transfer function

$$G_R(s) = \frac{1 + sT_n}{sT_i} \tag{3.1}$$

where $T_n = L_t / R_t$,

the filter inductance divided by the filter resistance [35]. This gives

$K_p = T_n / T_i$,

where T_i is the integral time constant and K_p is the proportional gain.

Inverter filter values are chosen to give a total harmonic distortion (THD) of close to 5% in the inverter output current, such that L_t = 0.04 mH and R_t = 0.004 Ω. This gives a T_n of 0.01, leaving the PI controllers for the d and q currents following the relationship of

$$K_p = \frac{0.01}{T_i} \tag{3.2}$$

The gains, as well as the DC voltage, are adjusted to keep the inverter in the linear region, where the amplitude modulation ratio m_a is less than one. K_p is selected to be 0.01, with the integral time constant of 1 second. The DC voltage is also increased to 18 kV to help generate the required levels of current.

Using the gains selected, a d axis current reference signal ($i_{\text{ref},d}$) is input into the controller, undergoing a step change from zero to 400 kA at t = 0.5 s. This gives a very fast rise time of 0.002 seconds for the inverter current i_d, going from zero to rated current as shown in Figure 3.7. A very similar response was seen for a step change in $i_{\text{ref},q}$.

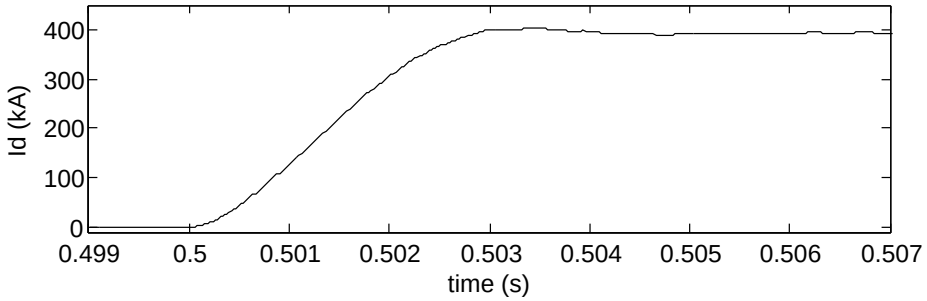

Figure 3.7 – Response of inverter current i_d to a step change in i_d reference current.

A filter is also added to the i_d and i_q inputs to the current controller to input a smoother signal into the controller. This is done using the real pole component in PSCAD, with a proportional gain of 1 and time constant of 0.0005 s. The decoupling components of the current controller ($\pm\omega L_t$ as shown in Figure 3.6) are removed from the design as they do not appear to improve performance.

As the inverter is only able to give a maximum i_d of 400 kA before overmodulation occurs (where $m_a > 1$), and a corresponding maximum power of 338 MW, six inverters will need to be used instead of one. This will still enable a maximum inverter power of 2000 MW. It will also be more realistic to have numerous inverters rather than just one aggregate inverter. It also opens the possibility of different control methods for different inverters.

3.3.3 PWM Design

As the only PWM component available within PSCAD is incorporated in the hysteresis current control PWM generator, a new PWM component is designed using FORTRAN. The control signals from the current controller are compared with a triangular carrier signal of frequency 2 kHz and amplitude of 1. This is used to generate the switching pulses for the inverter IGBTs.

3.3.4 Loop-Shaping

To tune the PI controllers for the inverter real and reactive power, the loop-shaping method is used as described in [36]. Loop-shaping is an optimisation approach to minimise the sum of the second norm of errors between the system open loop transfer function L and the desired open loop transfer function L_D. L is a combination of the plant transfer function G and the controller transfer function K such that

$$L(j\omega) = G(j\omega)K(j\omega). \tag{3.3}$$

To determine the optimal controller transfer function K, the plant transfer function G must first be determined. This can be done by determining the magnitude and phase of G over a suitable range of frequencies. One way to do this is to apply a pseudo-random binary sequence

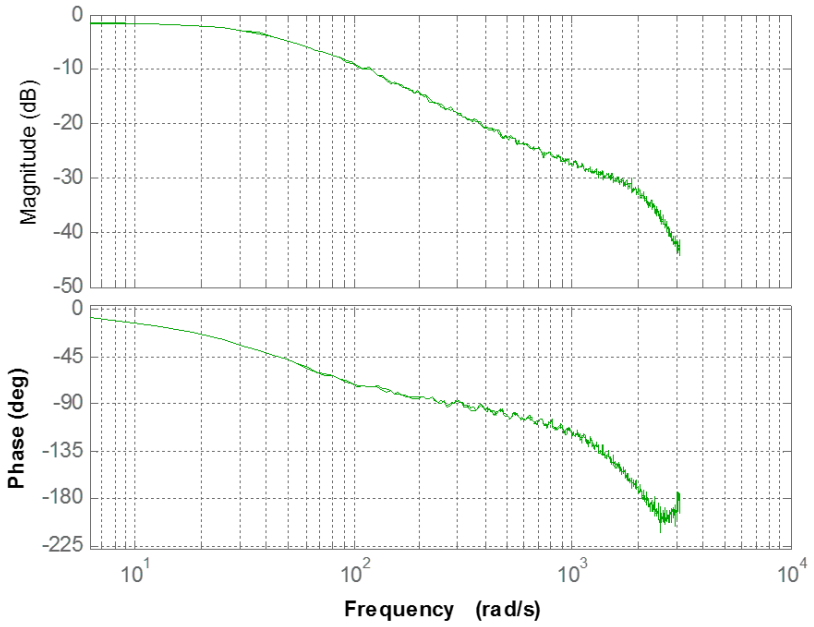

Figure 3.8 – Bode diagram of G (tuning P control).

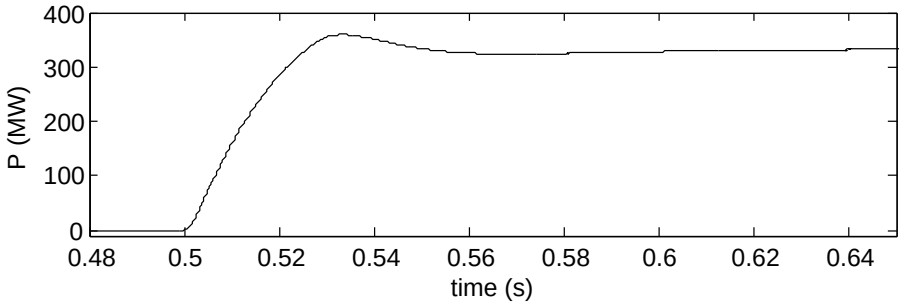

Figure 3.9 – Response of active power to step change in reference power.

or PRBS. These are rectangular waveforms with random width that have the properties of discreet time white noise.

A PRBS signal is generated in PSCAD with the use of a FORTRAN script. The signal has an amplitude of one and a $T_{s,id}$ of 1 ms, where the PRBS output is calculated to be either -1 or 1 every $T_{s,id}$. The signal repeats itself every 1023 $T_{s,id}$'s. The PRBS signal is input as the i_d reference in inverter simulations and the power is sampled every $T_{s,id}$. This is done for 20 PRBS cycles. The sampled power and i_d reference signals are then exported into MATLAB where an m-file is used to calculate G, which is shown on the bode diagram (Figure 3.8).

This is then input into the *condes* function, from a MATLAB toolbox, which calculates K using loop-shaping based on the desired open loop transfer function L_d [49]. As the goal is to have zero steady state error as well as satisfactory dynamic performance, the desired open loop

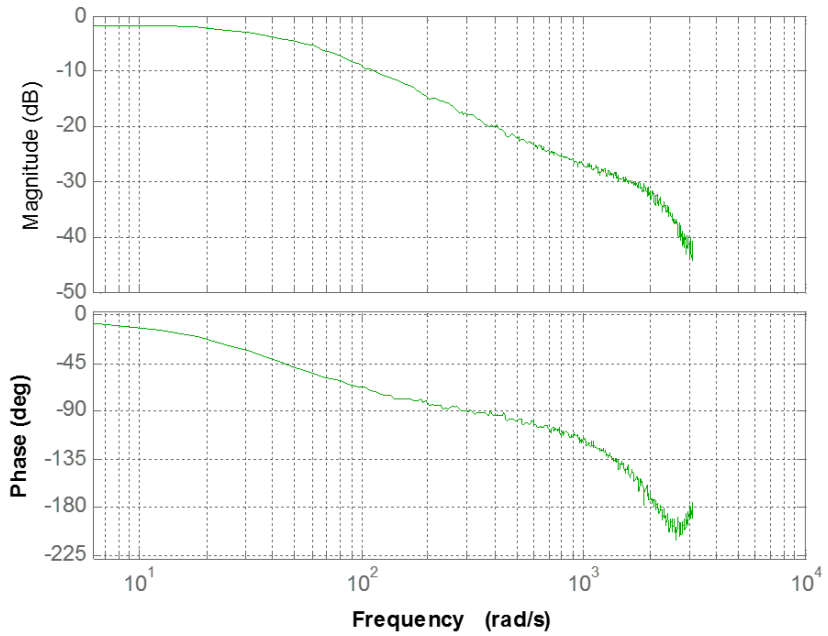

Figure 3.10 – Bode diagram of G (tuning Q control).

transfer function is chosen to be

$$L_d = \frac{\omega_c}{s}. \tag{3.4}$$

The cutoff frequency, ω_c, can then chosen to achieve the required dynamic performance. In this case ω_c is taken to be 100, which should give a rise time in response to a step change of approximately 10 ms.

Using the *condes* function, K is calculated to be

$$K = \frac{2.489(s+40.05)}{s}, \tag{3.5}$$

therefore giving a proportional gain of 2.489 and an integral time constant of 0.01 s. Using these values, a reference power signal was input into the PI controller, undergoing a step change from zero to 333 MW at 0.5 s. The rise time of the inverter from zero to rated power of 333 MW is close to 0.02 s as shown in Figure 3.9, demonstrating a fast response.

The PI controller for reactive power control is similarly tuned. Figure 3.10 shows the bode diagram for G.

This gives a K of

$$\frac{2.4075(s+45.92)}{s}. \tag{3.6}$$

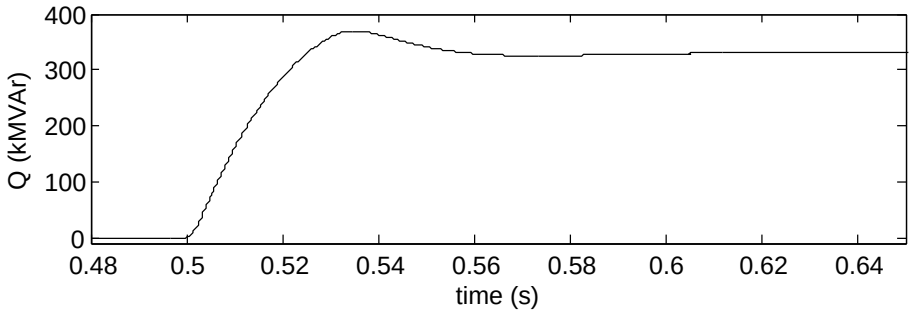

Figure 3.11 – Reactive power response to step change in reference reactive power.

Using a proportional gain of 2.4075 and integral time constant of 0.009 s gives a rise time in response to a step change in the reactive power reference of 0.02 s, as shown in Figure 3.11. This is very similar to the real power response in Figure 3.9.

3.3.5 Improved Response to Faults

To test the performance of the redesigned inverter control, six inverters with tuned PQ controllers are used in the PSCAD simulation representing the South Australian network and its link to Victoria. Simulations are run with inverter powers at 500 MW and 1900 MW. After running the simulation for 40 s, a 100 ms single phase to ground fault is added to the system, as in Section 3.2.

The response of the network to the fault, with the new inverter design compared with the previous inverter design with un-tuned inverter control, is shown in Figures 3.12 and 3.13. Looking at Figure 3.12, where the inverter is at 500 MW and synchronous machine at 1500 MW, large improvements can be seen in both the inverter active and reactive power. There is a significant reduction in the spikes in the real and reactive power from the inverter as well a large reduction in noise. Small improvements are also seen in the responses in the frequency, phase, RMS voltage, and the synchronous generator power.

When the inverter power is increased to 1900 MW (and synchronous generator power reduced to 100 MW) as in Figure 3.13, even more noticeable improvements can be seen in the response of the inverter real and reactive power to the fault. Interestingly, the synchronous generator power, frequency, phase, and RMS voltage also see large improvements.

Table 3.1 shows a comparison of the maximum and minimum peaks following the occurrence of the fault. Improvements can be seen with both the 500 MW and the 1900 MW inverter in the inverter active and reactive power, frequency, the synchronous generator power output, and the RMS voltage. These results show considerable improvement to network stability after improvements to the inverter controls were made.

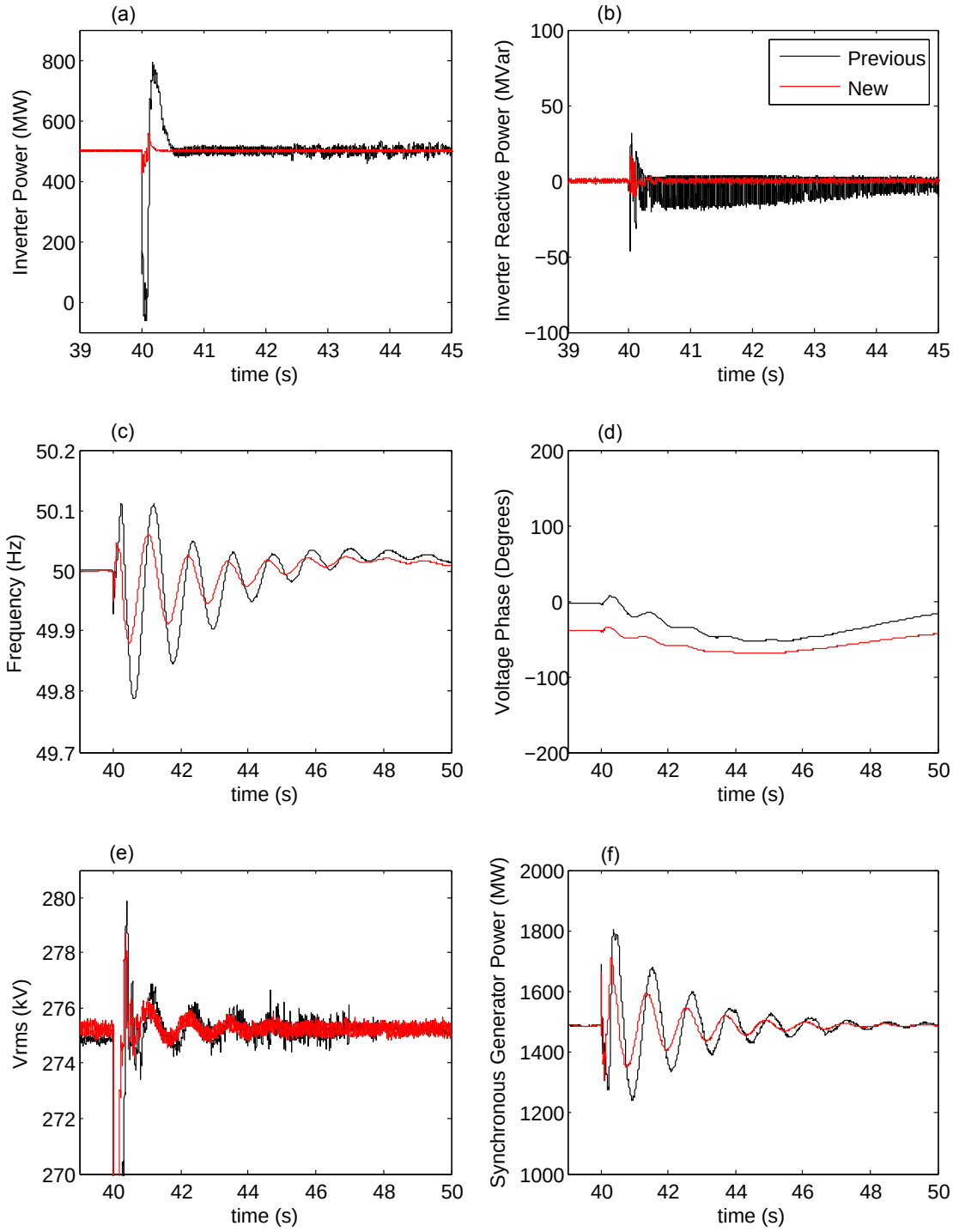

Figure 3.12 – Response after 100ms single phase to ground fault in a network with a 500 MW inverter comparing the new (red), and previous (black) inverter design control showing (a) inverter power (b) inverter reactive power (c) frequency (d) voltage phase angle line (e) RMS line to line voltage and (f) synchronous generator power.

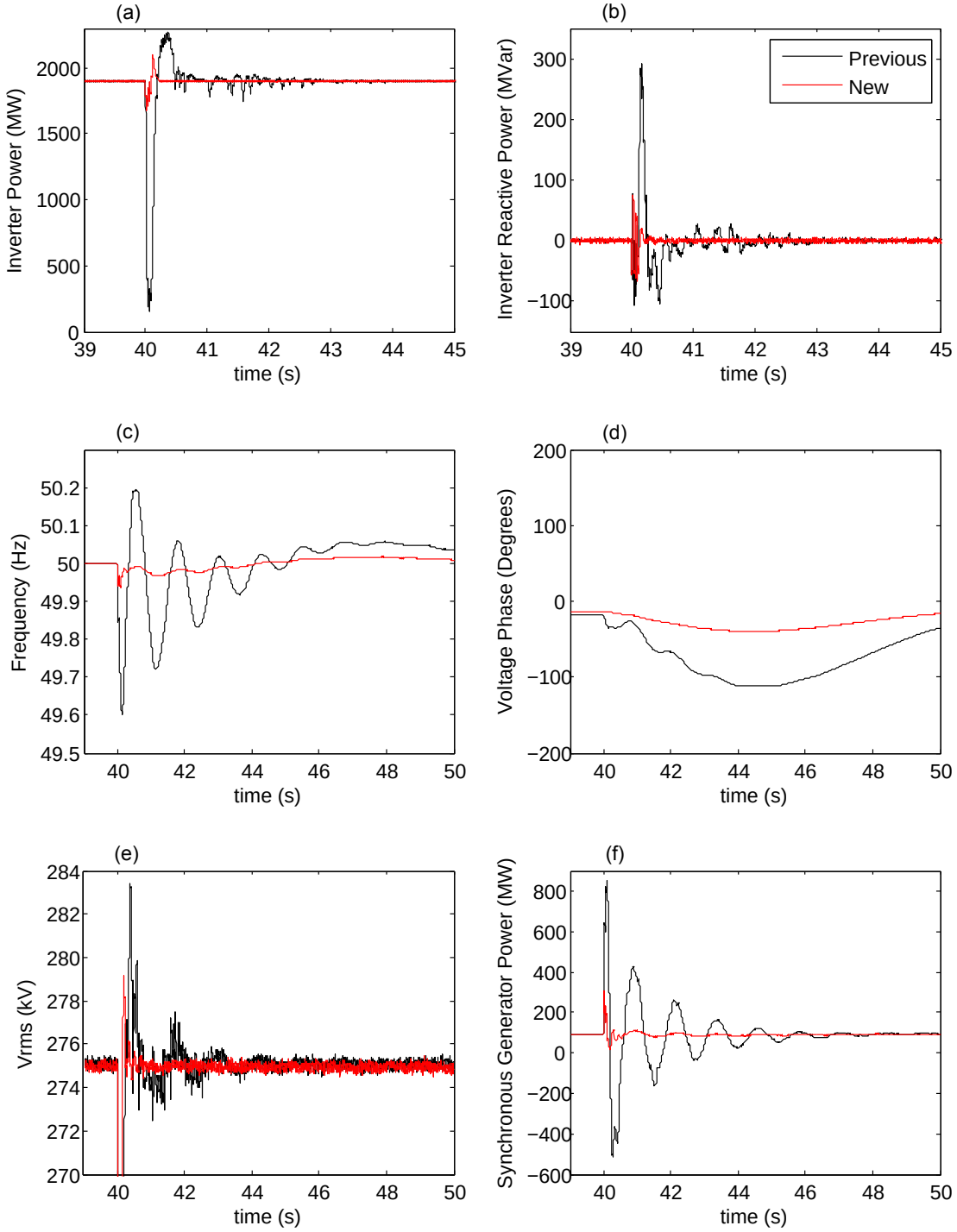

Figure 3.13 – Response after 100ms single phase to ground fault in a network with a 1900 MW inverter comparing the new (red), and previous (black) inverter design control showing (a) inverter power (b) inverter reactive power (c) frequency (d) voltage phase angle line (e) RMS line to line voltage and (f) synchronous generator power.

Table 3.1 – Comparison of the maximum and minimum peaks following a 100 ms single phase to ground fault before and after inverter control improvements.

		Maxiumum			Miniumum		
500 MW Inverter	**Nominal**	**Initial Inverter Control**	**Improved Inverter Control**	**Percentage Improvement**	**Initial Inverter Control**	**Improved Inverter Control**	**Percentage Improvement**
Inverter Power (MW)	500	793	556	81%	-61.1	420	86%
Inverter Reactive Power (MVAr)	0	31.3	16.8	46%	-46.0	-10.5	77%
Frequency (Hz)	50	50.11	50.06	46%	49.79	49.88	42%
SA Generator Power (MW)	1500	1806	1716	29%	1242	1306	25%
RMS Voltage (kV)	275	279.9	278.8	23%	150.8	190.5	32%
1900 MW Inverter	**Nominal**	**Initial Inverter Control**	**Improved Inverter Control**	**Percentage Improvement**	**Initial Inverter Control**	**Improved Inverter Control**	**Percentage Improvement**
Inverter Power (MW)	1900	2274	2096	47%	152	1677	87%
Inverter Reactive Power (MVAr)	0	291	76.1	74%	-108	-66.7	38%
Frequency (Hz)	50	50.20	50.02	91%	49.60	49.94	84%
SA Generator Power (MW)	100	849	310	72%	-513	16.2	86%
RMS Voltage (kV)	275	283.4	279.1	51%	164.2	208.1	40%

3.4 Governor Design

Initial simulations in Section 3.2 are run with a governor only on the larger 20,000 MW generator representing the external system. A constant level of torque is input into the 2000 MW generator on the South Australian side of the system. The reason for this is that when the governor models available in PSCAD are used on both generators, the governor on the smaller machine is not able to properly keep the generator at the required power of 2000 - X MW. Due to this issue, a separate governor is designed for the 2000 MW generator.

The governor and turbine design used is based on Hydro governor and turbine models available in Simulink as shown in Figure 3.14. The design used is based on PID control, with a speed error and a power error (or the servo motor output) being fed into the controller after being multiplied by a droop constant R_p. The signal is input into a servo motor model, which controls the hydro turbine. The turbine then determines the mechanical power input into the synchronous generator.

In PSCAD, a governor is designed based on this Simulink model. The design is shown in Figure 3.15. A PI controller is used instead of the PID and the internal loop option is replaced with the option to turn off the power control. The measured angular velocity ω is subtracted from the reference value (1 PU or $2\pi 50$ rad/s) to produce an error signal. The reference active power is also subtracted from the measured active power producing a power error signal, which is then multiplied by the droop constant, R_p (0.05 in this case). The two error signals for speed and power are then added together and input into a PI controller. The output of the PI controller is then input into a servo motor representation.

The servo motor is modelled as a second order system. The servo motor consists first of a real pole configuration, with an integral time constant T_A of 0.05 s and proportional gain of one. Next is the speed limiter, which limits the speed of the motor to $v_{\max}$ and $v_{\min}$ (± 0.16). Next

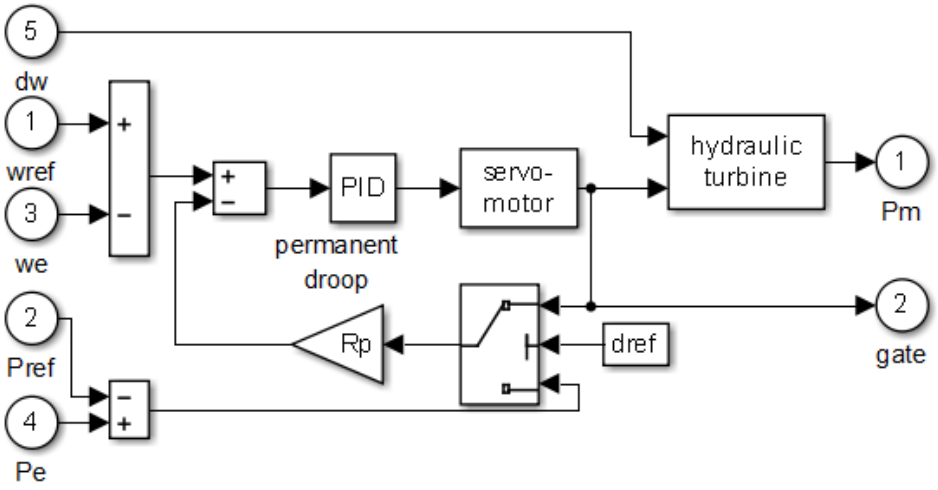

Figure 3.14 – Simulink hydro governor design [50].

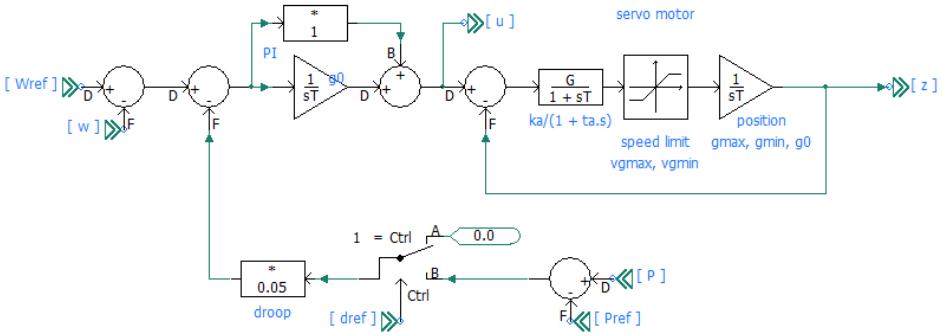

Figure 3.15 – Governor design.

is an integrator, which limits the position of the servo motor to g_{max} and g_{min}, followed by a feedback loop. The output from the servo motor is the turbine gate position z, which in input into the hydro turbine model. The turbine design, also based on the Simulink model, is shown in Figure 3.16.

Table 3.2 lists parameters used for the governor and turbine. Due to the duel inputs of both frequency and power error into the PI controller, loop-shaping has not able to be successfully used to tune the PI controller. Instead, proportional and integral gains are selected to give the best observed response.

3.5 Loads

When running simulations, it was realised that the induction motor load causes some problems. However, as it is unlikely that motor loads take up such a large proportion of the total load (initially one third), the proportion of the the induction motor is reduced to what is more realistically seen in a power system. Load proportions are altered by halving the induction

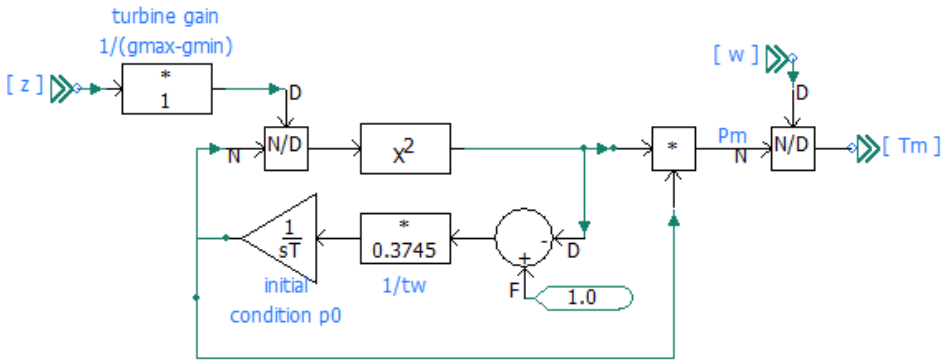

Figure 3.16 – Turbine design.

Table 3.2 – Governor and Turbine Parameters.

Proportional Gain (K_p)	1 (pu)
Integral Gain (K_i)	0.2 (pu)
Permanent Droop (R_P)	0.05 (pu)
Servomotor Time Constant (T_A)	0.05 (s)
Maximum Gate Opening (g_{max})	0.97518 (pu)
Minimum Gate Opening (g_{min})	0.01 (pu)
Speed Limit (vg_{max})	0.16 (pu/s)
Water Starting Time (t_w)	2.67 (s)

motor load, making it one sixth of the total load, or 250 MW. The remaining two loads are divided evenly between the remaining 1250 MW load power, 625 MW each.

3.6 Conclusions

A simplified representation of the South Australian electricity network is designed in PSCAD as described in Chapter 2. The purpose for designing this network is to test the stability of a power system as the proportion renewable generation (represented by an inverter) increases and synchronous generation decreases. Simulations are run at different levels of inverter penetration. For each inverter power level, simulations are run using three different types of inverter control: algebraic, PI control of active and reactive power, and PI control of active power and voltage. A single phase to ground fault is introduced to the network in order to test the stability.

According to the initial results, the stability of the network generally decreases as inverter penetration increases. There are, however, some exceptions seen in the synchronous generator power and the frequency responses which improve with increasing inverter penetration, except at very high inverter power levels. When comparing the different types of inverter control methods, both PI control of active and reactive power and algebraic give much better responses than PI control of active power and voltage.

Overall, the inverter control used in these simulations is quite lacking and improvements need to be made before any conclusions about network stability can be drawn. For better results, the PI inverter controls need to be properly tuned. For these simulations to accurately model the behaviour of synchronous machines, a governor also needs to be added to the aggregate synchronous generator model in the South Australian network representation.

In order to improve the network design, a number of improvements are made to the inverter. Improvements to the inverter inner current control loop are made by replacing the hysteresis current controller with a dq current controller. The outer control loops controlling active and reactive power are improved by using better-selected PI constants. The proportional and integral gains are optimised using the loop-shaping method. Simulation results show a considerable improvement in the response of the inverter to disturbances.

The design of a governor for the South Australian synchronous generator is also discussed. Load proportions are also altered to more realistically represent the proportion of induction motor loads in the network. After these improvements have been made, more accurate simulations can now be run to test the stability of a network at differing levels of inverter penetration.

In Chapter 4, the stability of the network will be evaluated using the network improvements made in this chapter. Network stability will be analysed at different inverter penetration levels in response to various faults applied to the network. The effect of inverter penetration, as well as the level of interconnector flow, will also be studied in the event of the disconnection of the Heywood Interconnector and the islanding of the South Australian Network.

4 Network Stability

4.1 Introduction

A simplified model of the South Australian electricity network, along with its connection to Victoria through the Heywood Interconnector, has been designed in PSCAD. The aim is to test the stability of the network in response to disturbances as the proportion of asynchronous generation increases within the network. This network design is discussed in Chapter 2. After some initial simulations were performed, it was realised that improvements needed to be made to the network. These improvements, discussed in Chapter 3, include improving the inverter control and designing a governor for the South Australian generator. With improved inverter tuning and governor control on the South Australian generator representation, simulations can now be run using a more accurate network model.

Simulations performed in Section 4.2 analyse the stability of the network in response to a 100 ms fault at varying levels of inverter penetration. The direction of the Heywood Interconnector power flow is also considered, with tests being done for power flow from South Australia to Victoria, as well as from Victoria to South Australia. A single phase fault is applied to a 275 kV bus in South Australia in a similar manner to what is done in Chapter 3. Different levels of inverter penetration are investigated, with inverter powers of 500, 1200 and 1900 MW tested.

Following this, in Section 4.3, a fault is then applied to one of the two parallel interconnector lines, causing one of the lines to trip. Initially, this is done as a 100 ms single phase to ground fault. To then test for a worse case, a 120 ms two phase to ground fault is simulated. As before, three different inverter penetration levels are tested, as are differing directions of interconnector power flow.

In Section 4.4, simulations are also performed to test the stability of the network following the complete disconnection of the Heywood Interconnector, disconnecting the South Australian network from the rest of Australia. Simulations are run at varying levels of power flow across

the interconnector, as well as at different inverter power levels. Finally, a discussion of the of the limitations of these studies is included in Section 4.5.

4.2 Response to Faults

To begin with, the South Australian network representation in PSCAD is subjected to a single phase fault. This is done in order to test the stability of the network at different inverter penetrations. The transient stability of the network is tested, making sure that synchronous generators remain synchronised with the network. Steady state frequency also needs to remain within the normal operating band of 49.85 to 50.15 Hz. For a network disturbance, operating standards state that the frequency be contained within 49 to 51 Hz, stabilised between 49.5 to 50.5 Hz within one minute, then returned back to the normal operating band within five minutes [48]. It is also important from the customers perceptive to avoid under frequency load shedding, which occurs if the frequency falls below 49 Hz [51]. Network voltages also need to be returned to the normal range of 0.9 to 1.1 PU after the disturbance [47].

To test the stability of the South Australian network at different inverter penetrations, a fault is applied to the network in a manner similar to that described in Chapter 3, Section 3.2. This time, however, a more realistic PSCAD network representation of the South Australian network is used, with a governor designed for the 2000 MW generator representing the synchronous generation within South Australia. The inverter, representing the asynchronous generation within South Australia, is now operating with better tuned PI control of active and reactive power.

When running the simulations, a 5 μs solution time step is used. Simulations are run for 70 s, with the fault occurring at t = 50 s. A single phase to ground fault is applied for 100 ms seconds on the 275 kV bus at the connection point for the inverter and loads on the South Australian side of the network, after which all lines are restored. As before, the fault impedance to ground is 0.01 Ω.

Simulations are run with inverter powers of 500, 1200, and 1900 MW. With the total generation in the South Australian network kept at 2000 MW, the remaining synchronous generator powers are set to 1500, 800, and 100 MW. Initially, the power flow on across the Heywood Interconnector is set at 500 MW flowing from South Australia to Victoria. The total load in South Australia is therefore absorbing 1500 MW. Simulation results are shown in Figure 4.1, which compares the response to the fault at the three different inverter power levels. The power flow across the interconnector is then reversed in direction, with 500 MW being transferred from Victoria to South Australia. Results for this scenario are seen in Figure 4.2.

4.2.1 Effect of Inverter Penetration

Looking Figures 4.1 and 4.2, there appears to be very little difference between the simulations run at different inverter penetration levels. The response seen in the synchronous generator power does appear to be less severe as the inverter size increases. However, this is understandable when the small synchronous generator sizes are taken into consideration. Similarly, the responses seen in the inverter active and reactive power during and after the fault also seems reduced when inverter size decreases. The RMS voltage measurements after the fault are nearly identical for all three inverter penetration levels. The response in the frequency is also very similar for all inverter powers, with the small differences most likely due to the slightly different steady state frequency levels before the fault occurs. This is also observed when looking at the phase angle.

When considering the forward and reverse power flow directions across the Heywood Interconnector, there seems to be a lower nadir in the frequency when power is flowing towards South Australia. Overall, the frequency remains within the normal operating band both during and following the fault for both power flow directions, and at each inverter penetration level tested. Voltage returns quickly to its steady state value of 275 kV, within a time period of 1 second. This satisfies both frequency and voltage stability requirements. Angle stability is also satisfied with synchronous machines remaining synchronised with the grid.

This result suggests that increasing inverter penetration levels in this simplified version of the South Australian network does not cause any loss of stability within the network. To further test if this conclusion is accurate, more severe disturbances in this network are analysed in the next sections.

4.3 Line Trip Simulations

To examine what would happen when a more severe disturbance occurs in the network, simulations are run to observe what happens when one of the two parallel interconnector lines is taken out of service. As before, the stability of the network is compared at three different inverter penetration levels. The frequency and voltage stability must again be maintained, as must the rotor angle stability of the synchronous generators.

4.3.1 Single Phase Fault

In these simulations, after initially running for 50 seconds to make sure the network achieves steady state, a single phase to ground fault is added to one of the Heywood Interconnector lines on the South Australian side. After the fault is applied for 100 ms the line is tripped, leaving only a single interconnector line in service, rather than the usual two. The simulation is then continued with the line out of service until t = 100 s. Simulations are run with inverter powers of 500, 1200, and 1900 MW. The power flow across the Heywood Interconnector is initially set

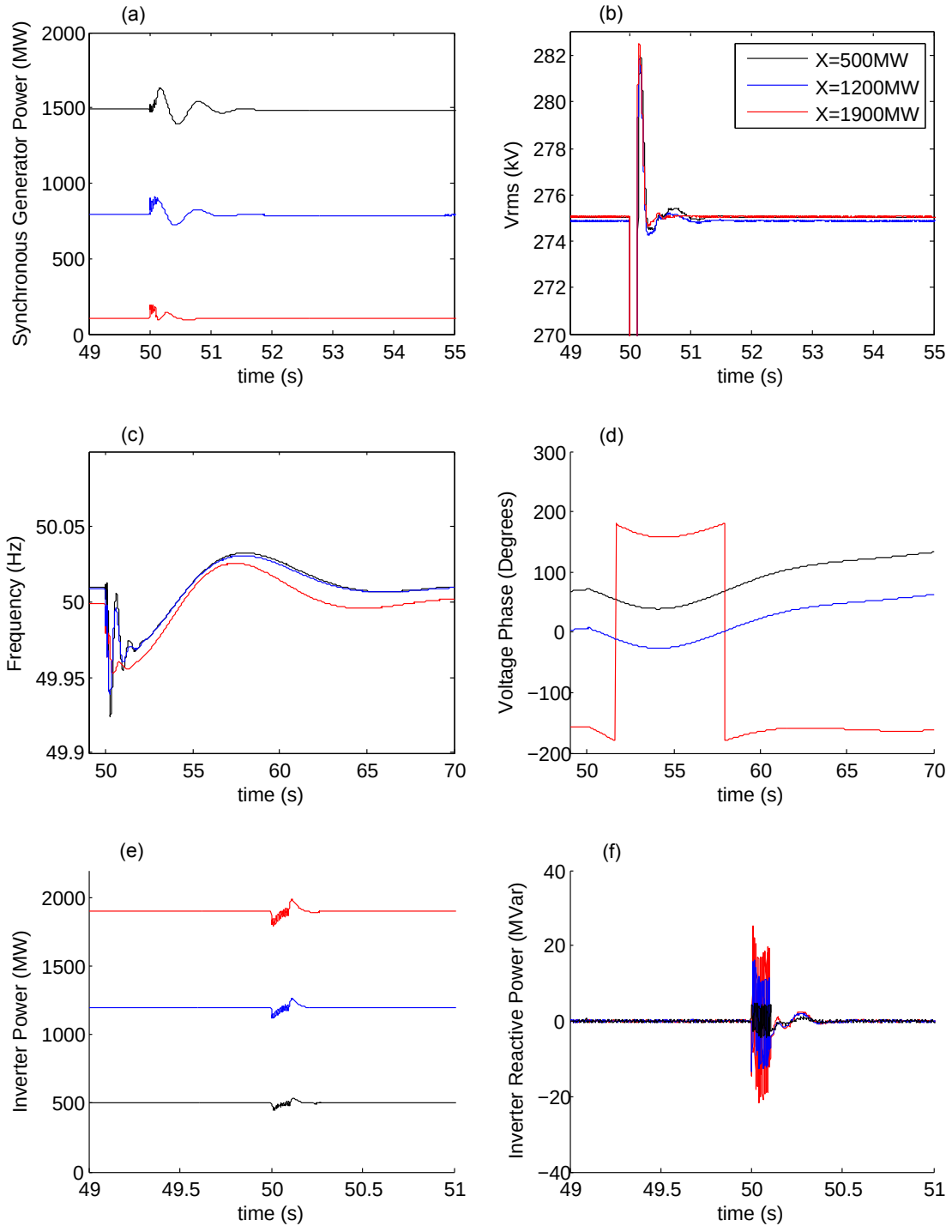

Figure 4.1 – Response after 100ms single phase to ground fault in a network with a 500 MW inverter (black), 1200 MW inverter (blue), and a 1900 MW inverter (red) using P and Q PI control showing (a) synchronous generator power (b) RMS line to line voltage (c) frequency (d) voltage phase angle (e) inverter power and (f) inverter reactive power. Heywood Interconnector flow is 500 MW to Victoria.

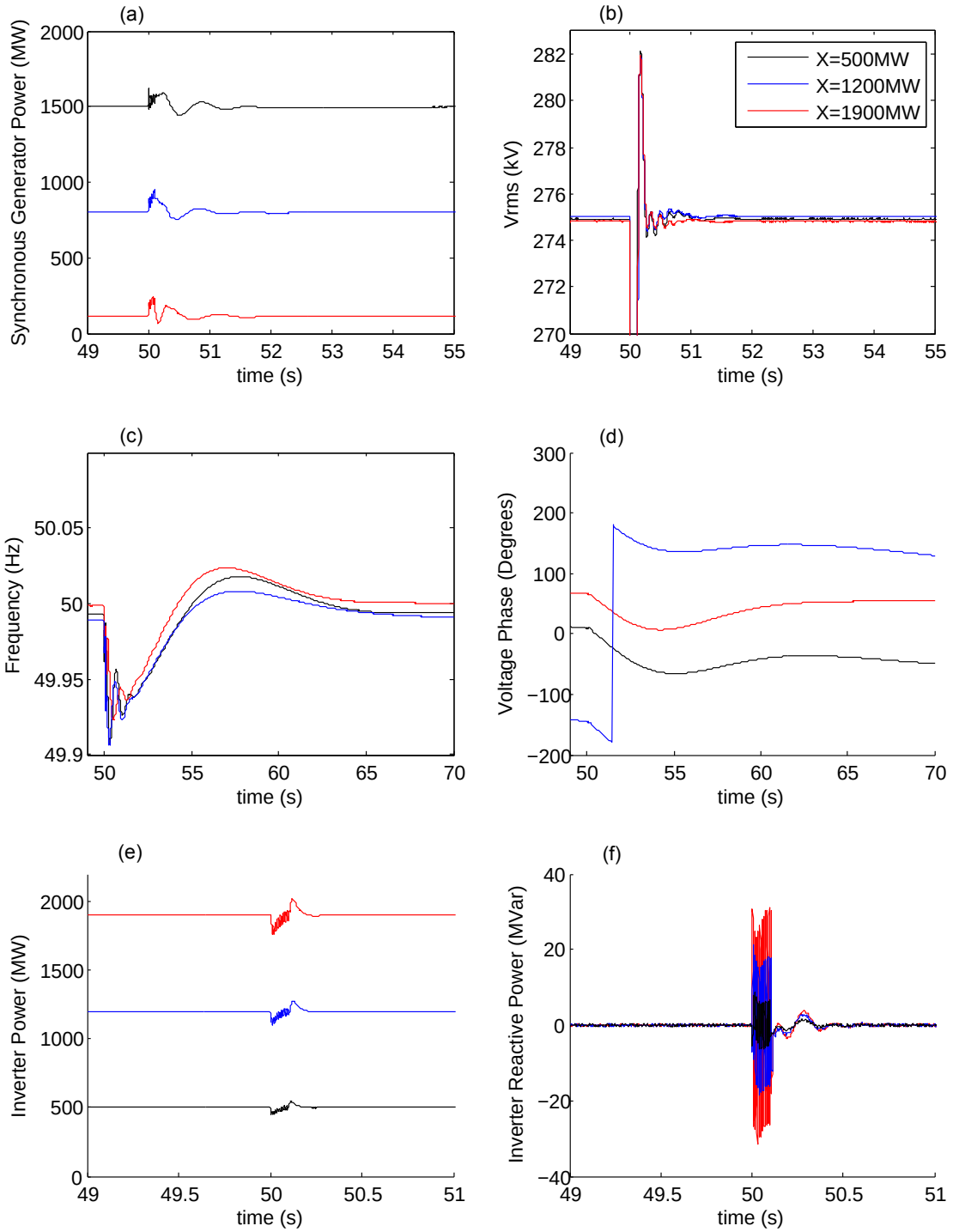

Figure 4.2 – Response after 100ms single phase to ground fault in a network with a 500 MW inverter (black), 1200 MW inverter (blue), and a 1900 MW inverter (red) using P and Q PI control showing (a) synchronous generator power (b) RMS line to line voltage (c) frequency (d) voltage phase angle (e) inverter power and (f) inverter reactive power. Heywood Interconnector flow is 500 MW to South Australia.

at 500 MW flowing from South Australia to Victoria. The resulting network response is shown in Figure 4.3. The power flow across the link is then reversed in direction, with 500 MW being transferred from Victoria to South Australia. These results can be seen in Figure 4.4.

Examining Figures 4.3 and 4.4, there is still very little difference seen between the three inverter penetration levels. Again, the response seen in the inverter active and reactive power is slightly worse at higher inverter power levels. This is expected with the response in the inverter being proportional to its size. Very slight differences are seen in frequency, voltage phase angle, and RMS voltage at different inverter penetrations, with the small differences most likely due to slight variations in their starting steady state positions. Not a lot difference is observed in synchronous generator power at different inverter penetrations either. When the power flow across the interconnector is flowing into South Australia (Figure 4.3) rather than away from South Australia (Figure 4.4), there is a slightly larger drop in frequency. However, it should be noted that even during the disturbance the frequency remains in the normal operating band of 49.85 to 50.15 Hz.

At all inverter penetrations stability requirements are met, with frequency remaining within the normal operating band and steady state voltage only dropping by at most one percent from its nominal value. There is still very little difference seen in network stability as inverter penetration increases in the network.

4.3.2 Two Phase Fault

Following these simulations, a two phase fault is applied to see if any difference can be found between different inverter penetrations under a more severe disturbance. A two phase fault is chosen rather than a three phase fault due to the fact that three phase faults are much more unlikely occurrences. AEMO also does not consider three phase faults to be credible contingency events [52].

After running the simulation for 50 seconds to get to steady state, a two phase to ground fault is applied to one of the two parallel Heywood Interconnector lines on the South Australian side. In this case, the fault is sustained for 120 ms, rather than the 100 ms in previous cases. After this the interconnector line is tripped, leaving only one line remaining. The simulation is then continued with the line out of service until t = 100 s. Simulations are run at inverter powers of 500, 1200, and 1900 MW. Figure 4.5 shows the network response to the fault with 500 MW of power flowing from South Australia to Victoria, while Figure 4.6 is with 500 MW being transferred from Victoria to South Australia.

Looking at the results, it appears that when the inverter power is increased to 1900 MW, large spikes are seen in the inverter active and reactive power, as well as the RMS voltage. Although, these do occur on a time scale of under 500 ms. There are also much larger oscillations seen in the synchronous generator as a response to the disturbance. The best response for the synchronous generator is seen at 1200 MW inverter penetration. Little difference is seen in the

responses in the frequency and the phase at different inverter power levels. There does appear to be a slightly larger drop in frequency when inverter power is at 500 MW compared to 1200 and 1900 MW inverter powers.

Although there are larger oscillations this time in the synchronous generator power, these are damped within a few seconds. Voltage stability has been satisfied with voltage levels returning to near nominal levels within seconds. When the Heywood Interconnector power is flowing into Victoria, frequency remains above 49.5 Hz, retuning to the normal operating range within a few seconds, satisfying frequency stability requirements. In the case of power flow into South Australia, the frequency does fall very briefly below 49.5 Hz (for the 500 MW inverter case). It returns to the 49.5 to 50.5 Hz boundary well within one minute and back to the normal operating band well within the five minutes required by the frequency operating standards. The time scales here occur within seconds rather than minutes. In all cases, the synchronous machines still maintain rotor angle stability to satisfy stability requirements.

These result still tend to show that increasing the inverter penetration in this PSCAD model of the South Australian network does not negatively affect the stability within the network. While this may be true so far for disturbances occurring within the network, another relevant event that needs to be studied is the islanding of the South Australian network. The effect of disconnecting the Heywood Interconnector, separating the only AC connection from South Australia to Victoria, is studied in Section 4.4.

4.4 Heywood Interconnector Disconnection

In recent years, the tripping of the Heywood Interconnector has caused problems for the South Australian electricity network. On the 28th of September 2016 the Heywood Interconnector was tripped following a series of events that ultimately resulted in a black system [42]. A fault also caused the loss of the interconnector on the 1st of December 2016. This resulted in under frequency load shedding, with 703 MW of customer load lost [51].

In this section, the stability of the network is tested at different inverter penetration levels following the disconnection of the Heywood Interconnector. As in the previous sections, frequency and voltage stability are tested. For a separation event that forms an island, the NEM mainland frequency operating standards state that frequency must be contained within 49 to 51 Hz, stabilised between 49.5 and 50.5 Hz within 2 minutes and and 49.85 to 50.15Hz within 10 minutes [48].

Simulations are run with inverter powers of 500, 900, and 1200 MW, with the South Australian synchronous generator powers set at 1500, 1100, and 800 MW. The total generation within South Australia is therefore set at 2000 MW. The synchronous generator powers are chosen to allow movement of ±500 MW generated, to allow compensation following the loss of the Interconnector. Simulations are initially run for 50 seconds to allow the network to reach steady state. After this, a 100 ms single phase to ground fault occurs, followed by the tripping

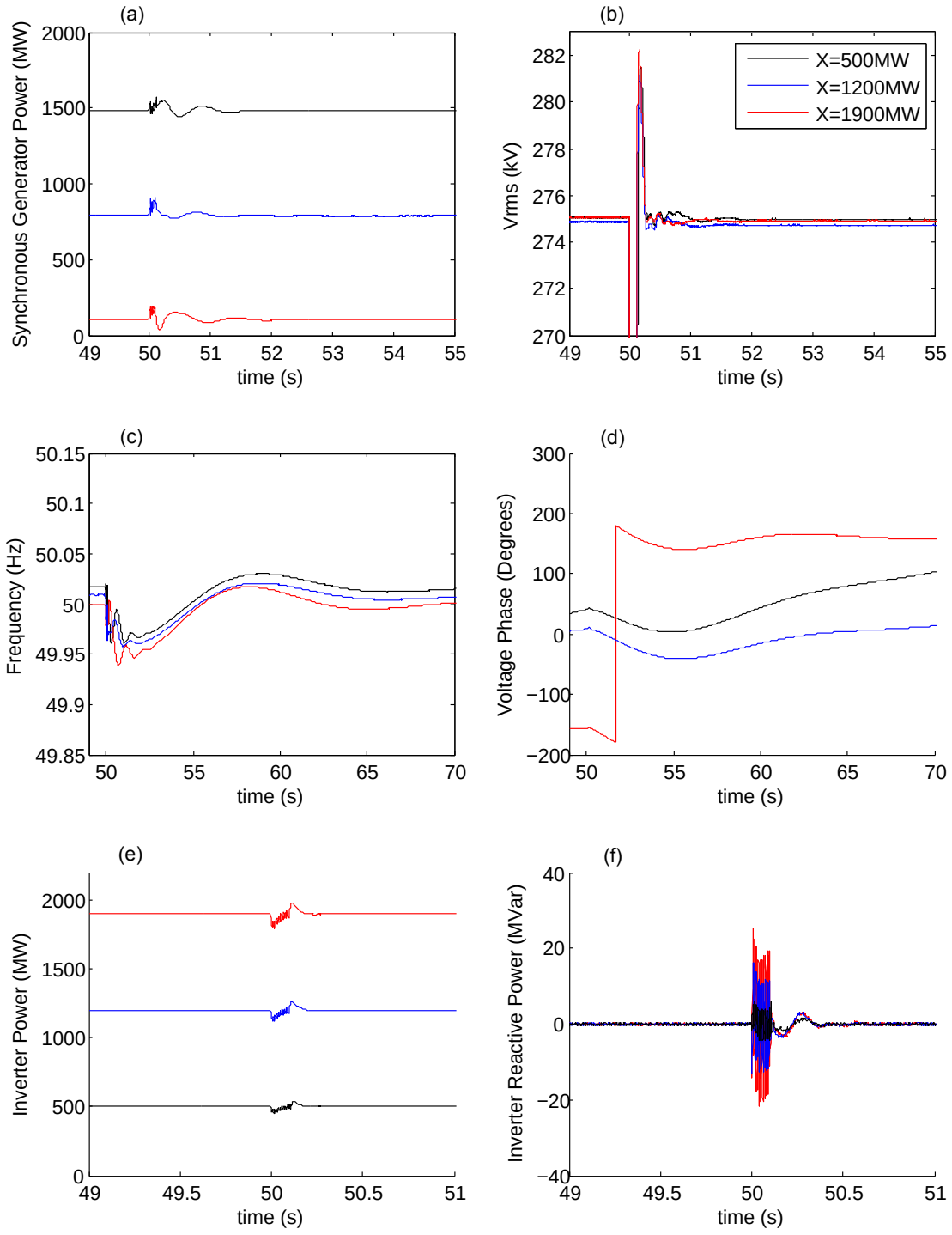

Figure 4.3 – Response after 100ms single phase to ground fault with a single interconnector line tripped in a network with a 500 MW inverter (black), 1200 MW inverter (blue), and a 1900 MW inverter (red) using P and Q PI control showing (a) synchronous generator power (b) RMS line to line voltage (c) frequency (d) voltage phase angle (e) inverter power and (f) inverter reactive power. Heywood Interconnector flow is 500 MW to Victoria.

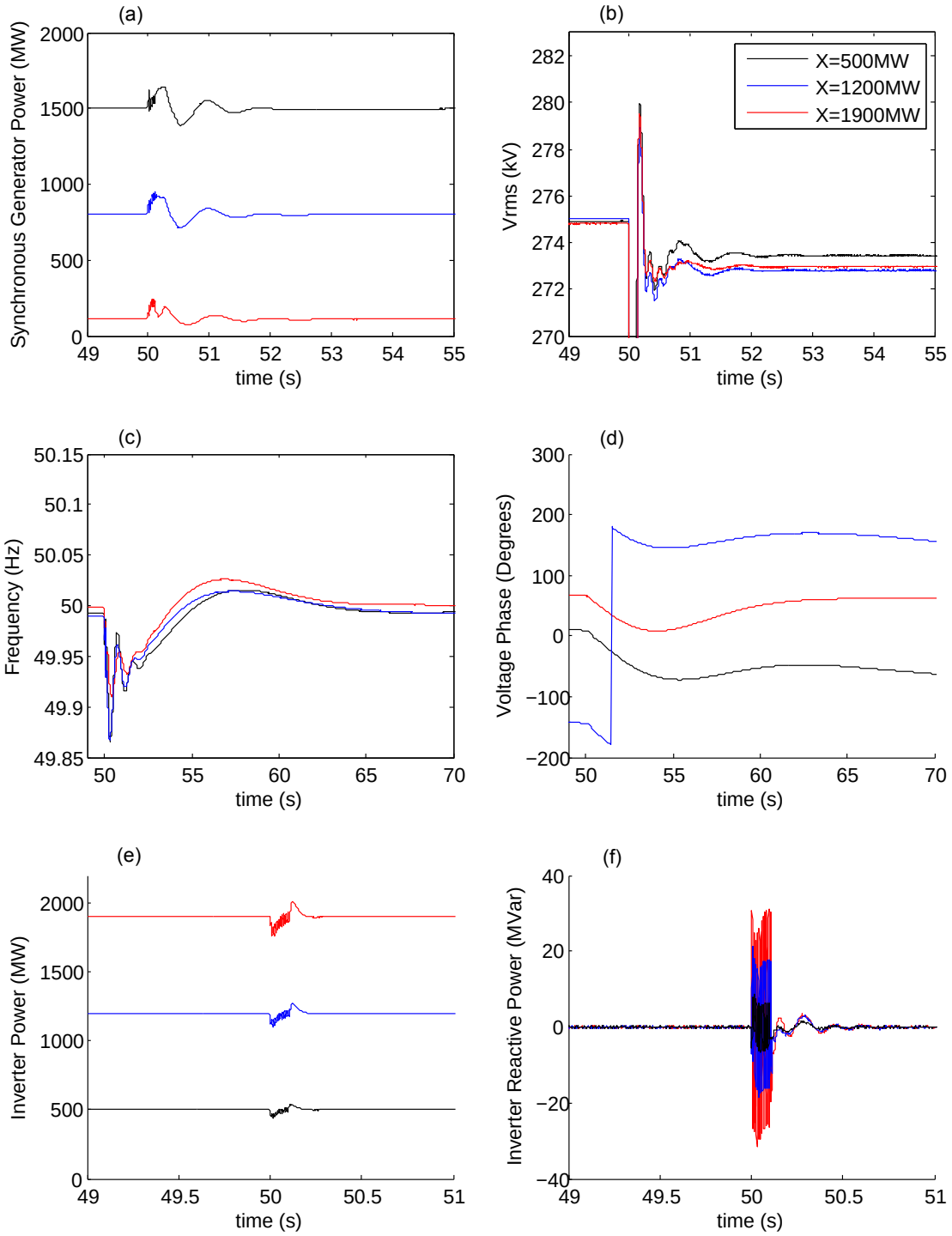

Figure 4.4 – Response after 100ms single phase to ground fault with a single interconnector line tripped in a network with a 500 MW inverter (black), 1200 MW inverter (blue), and a 1900 MW inverter (red) using P and Q PI control showing (a) synchronous generator power (b) RMS line to line voltage (c) frequency (d) voltage phase angle (e) inverter power and (f) inverter reactive power. Heywood Interconnector flow is 500 MW to South Australia.

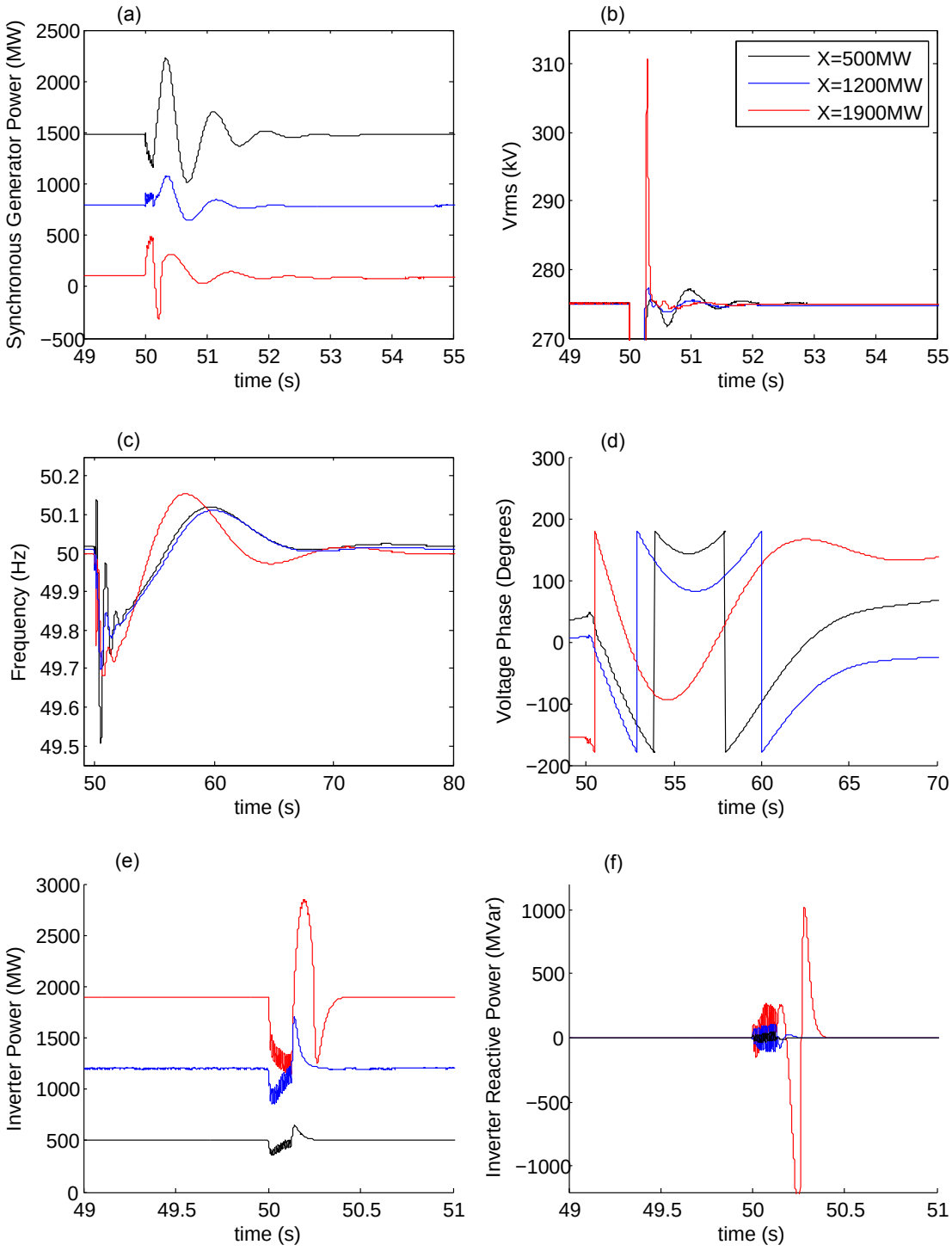

Figure 4.5 – Response after 120ms 2 phase to ground fault with a single interconnector line tripped in a network with a 500 MW inverter (black), 1200 MW inverter (blue), and a 1900 MW inverter (red) using P and Q PI control showing (a) synchronous generator power (b) RMS line to line voltage (c) frequency (d) voltage phase angle (e) inverter power and (f) inverter reactive power. Heywood Interconnector flow is 500 MW to Victoria.

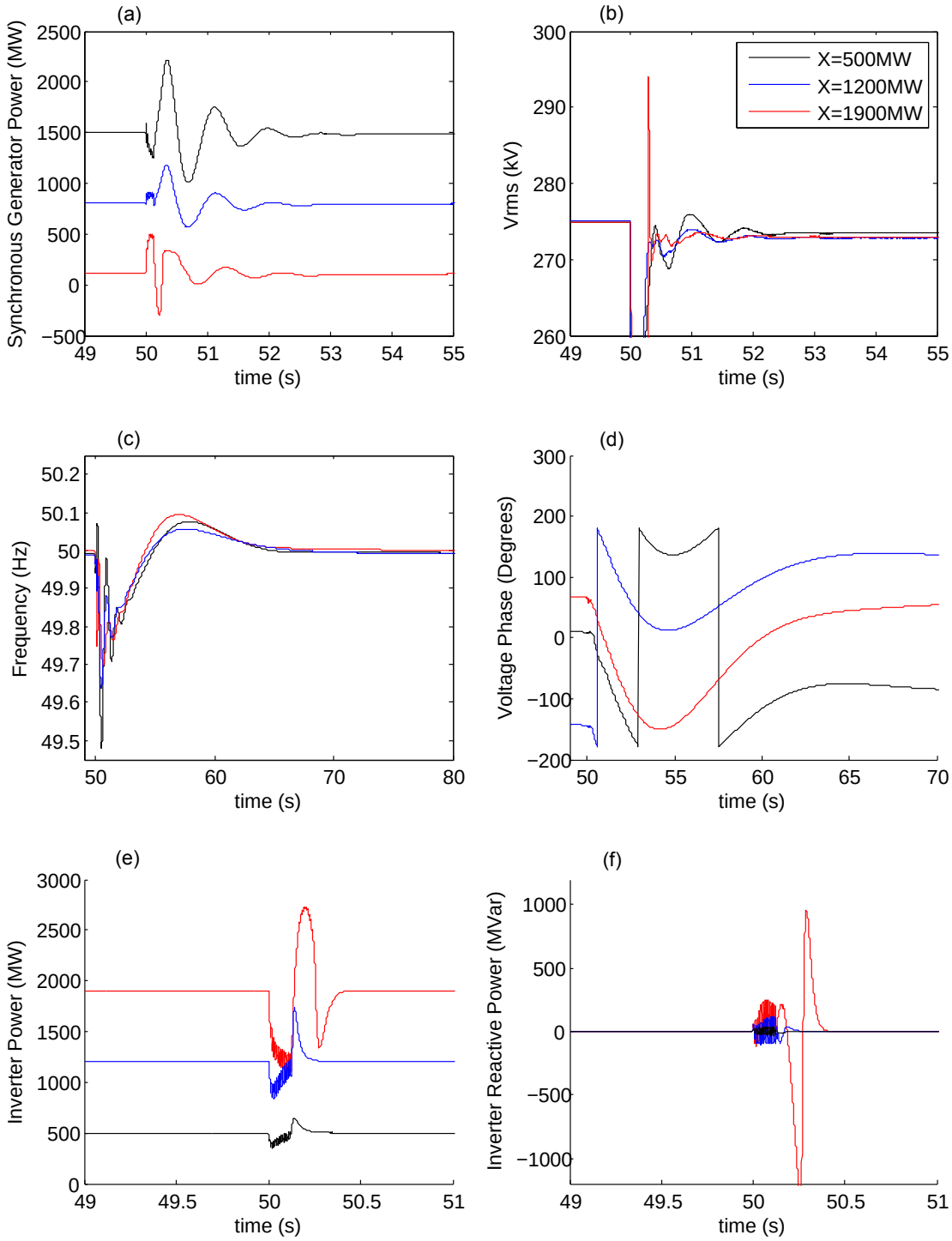

Figure 4.6 – Response after 120ms 2 phase to ground fault with a single interconnector line tripped in a network with a 500 MW inverter (black), 1200 MW inverter (blue), and a 1900 MW inverter (red) using P and Q PI control showing (a) synchronous generator power (b) RMS line to line voltage (c) frequency (d) voltage phase angle (e) inverter power and (f) inverter reactive power. Heywood Interconnector flow is 500 MW to South Australia.

of the two parallel lines representing the Heywood Interconnector. The simulation is then continued until t = 100 s. At the time of the interconnector trip, the governor of the South Australian synchronous generator is switched to frequency control only. A 5 μs solution time step is used when running simulations.

Four scenarios of interconnector flow are analysed: 200 MW to Victoria, 200 MW to South Australia, 500 MW to Victoria, and 500 MW to South Australia. Simulations results are shown in Figures 4.7 to 4.10, which compare the response of the South Australian network to the network fault followed by the trip of the Heywood Interconnector, comparing the three different inverter penetration levels.

4.4.1 200 MW Interconnector Flow

The 200 MW interconnector flow case, with 200 MW flowing into Victoria, is shown in Figure 4.7. The South Australian synchronous generator power can be seen to drop by 200 MW to compensate for the loss of load across the interconnector. While for all three different inverter power levels the voltage recovers to slightly below the steady state, the voltage drop gets larger as inverter penetration level increases. For frequency, on the other hand, the response improves as inverter penetration increases, with lower frequency deviation above 50 Hz. Not much difference is seen in the inverter active and reactive power responses. Figure 4.8 shows the response to the Heywood interconnector trip for the case of 200 MW of power flow into South Australia. The most significant difference is seen when looking at the response in the frequency. Again, it appears that a larger inverter penetration improves stability, as the frequency drop is less severe and the recovery is faster.

4.4.2 500 MW Interconnector Flow

For the scenarios with higher flow across the Heywood Interconnector, Figure 4.9 shows the Heywood Interconnector Trip with 500 MW of power flow into Victoria while Figure 4.10 is for 500 MW of power flow into South Australia. Again the same pattern is seen with larger deviations from the 50 Hz frequency after the trip and slower recovery times as the proportion of power generated by inverters decreases. The worst case is for the 500 MW inverter with 500 MW interconnector power flow into South Australia (Figure 4.10). In this case frequency does not return to 50 Hz but instead settles at 44 Hz, which is not an acceptable outcome when it comes to frequency stability.

In many of these cases, the frequency falls below 49 Hz, which would in reality trigger load shedding. It is also quite possible that the aggregate representations of the synchronous machines do not accurately represent how these machines and their governors respond to disturbances. These and other limitations of this work are discussed in Section 4.5. Even so, these results indicate that increasing inverter penetration does not necessarily reduce the stability of a network, and can in some cases may even improve stability.

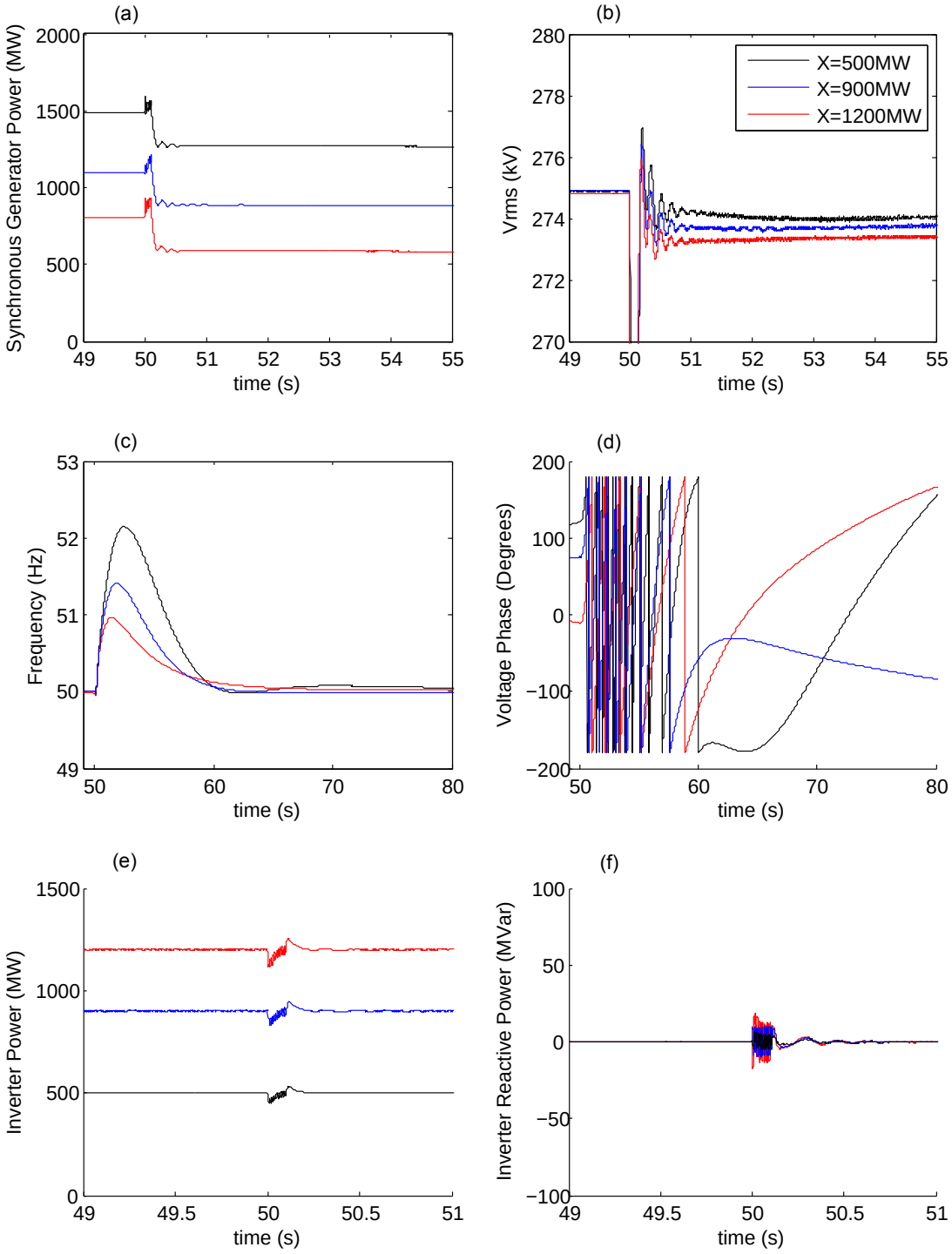

Figure 4.7 – Response after 100ms single phase to ground fault followed by an Interconnector trip in a network with a 500 MW inverter (black), 900 MW inverter (blue), and a 1200 MW inverter (red) showing (a) synchronous generator power (b) RMS line to line voltage (c) frequency (d) voltage phase angle (e) inverter power and (f) inverter reactive power. Heywood Interconnector flow is 200 MW to Victoria.

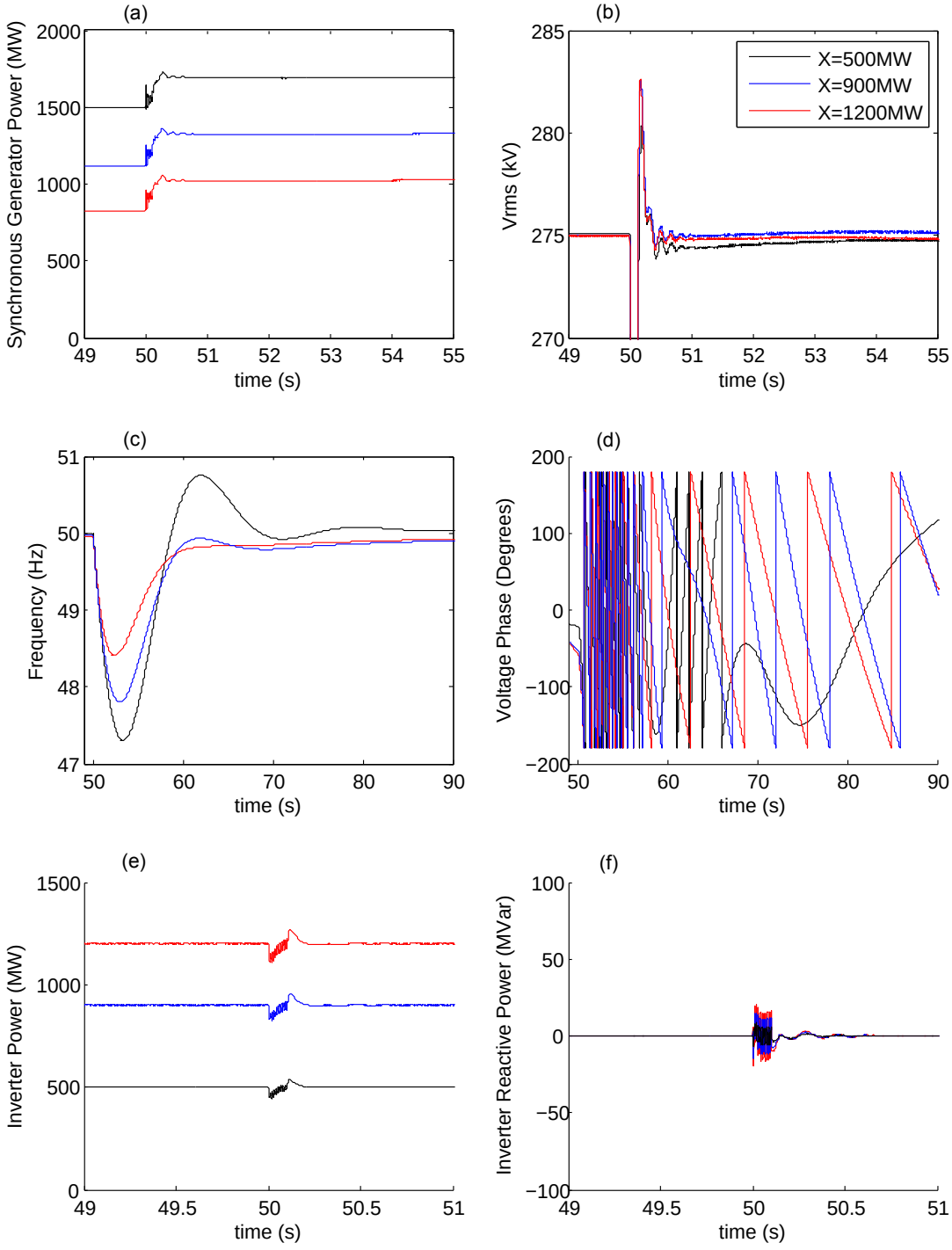

Figure 4.8 – Response after 100ms single phase to ground fault followed by an Interconnector trip in a network with a 500 MW inverter (black), 900 MW inverter (blue), and a 1200 MW inverter (red) showing (a) synchronous generator power (b) RMS line to line voltage (c) frequency (d) voltage phase angle (e) inverter power and (f) inverter reactive power. Heywood Interconnector flow is 200 MW to South Australia.

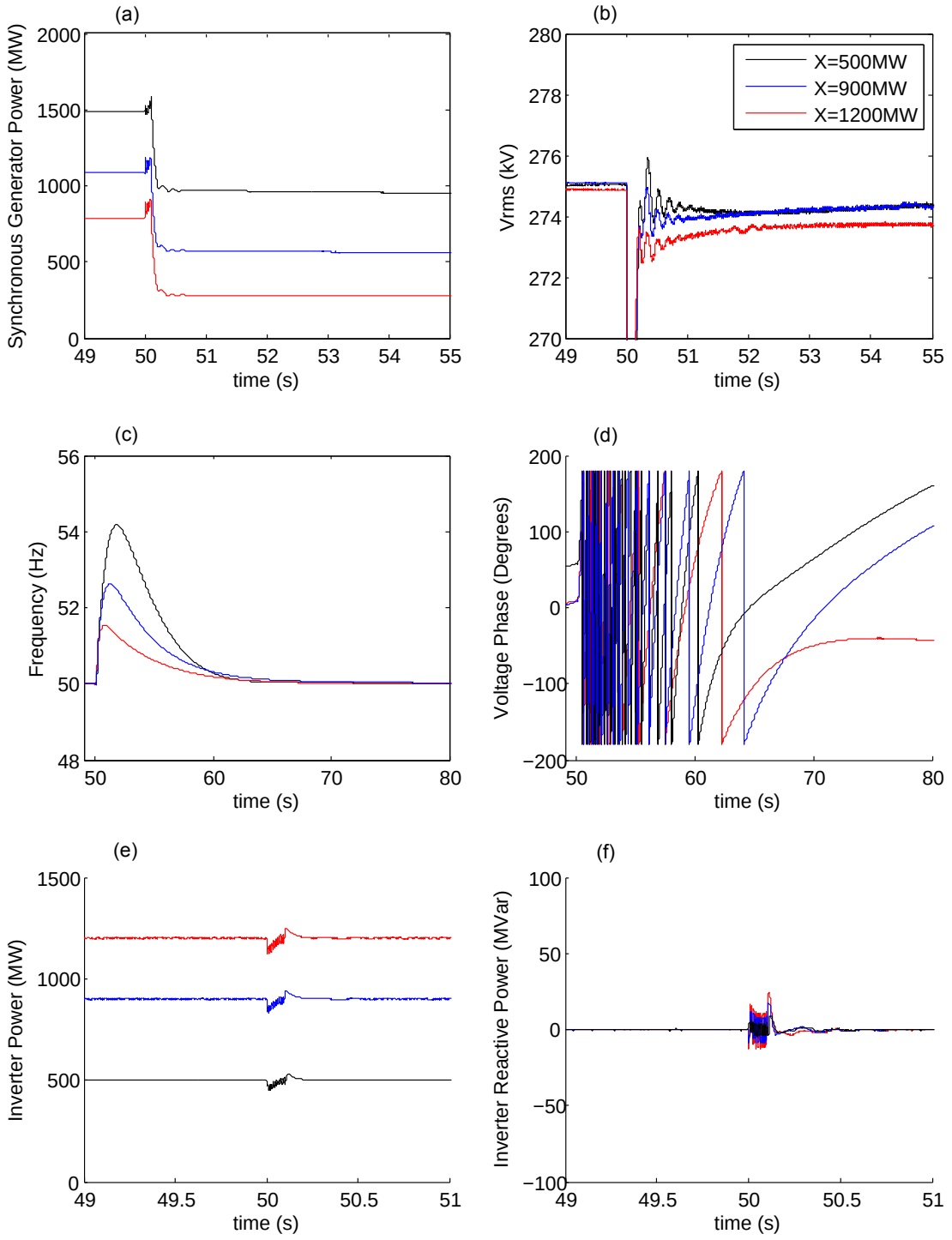

Figure 4.9 – Response after 100ms single phase to ground fault followed by an Interconnector trip in a network with a 500 MW inverter (black), 900 MW inverter (blue), and a 1200 MW inverter (red) showing (a) synchronous generator power (b) RMS line to line voltage (c) frequency (d) voltage phase angle (e) inverter power and (f) inverter reactive power. Heywood Interconnector flow is 500 MW to Victoria.

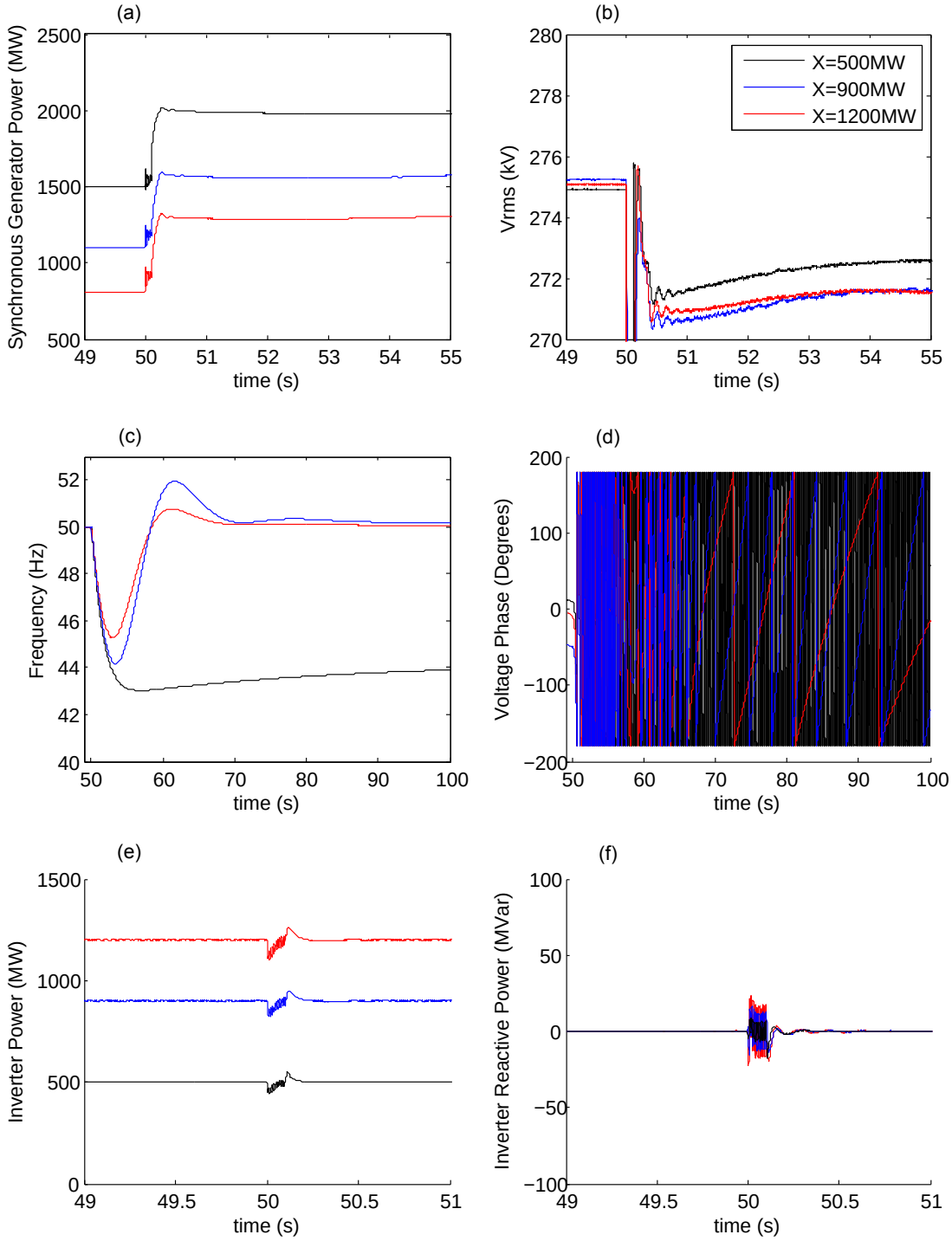

Figure 4.10 – Response after 100ms single phase to ground fault followed by an Interconnector trip in a network with a 500 MW inverter (black), 900 MW inverter (blue), and a 1200 MW inverter (red) showing (a) synchronous generator power (b) RMS line to line voltage (c) frequency (d) voltage phase angle (e) inverter power and (f) inverter reactive power. Heywood Interconnector flow is 500 MW to South Australia.

4.4.3 Importance of Governors

There have been recent concerns within the NEM that the use of primary frequency control has declined since the introduction of the FCAS market [43, 44]. A recent report has found that more and more generators are turning off their governors, or setting very wide dead bands, in order to meet dispatch targets [44]. This means that the modelling done in this thesis, with a governor on the synchronous generator representing all the synchronous generation within South Australia, may not be actually what is happening in reality.

To briefly look at the impact of the presence of synchronous generator governors, two identical simulations are performed both with and without governors present in South Australia. This is tested with the 900 MW inverter power simulation described in Section 4.4 (Figure 4.9), with 500 MW of power flowing over the interconnector towards Victoria. With no governor, the turbine is set to run to provide a constant 1100 MW. As before, the simulation is run for 50 s after which a 100 ms single phase to ground fault occurs next to the interconnector. This is followed by a trip of the two parallel lines of the Heywood Interconnector, after which the simulation is run for a further 50 s. At the same time as the interconnector is tripped, the South Australian synchronous generator power set-point is dropped by 500 MW to 600 MW, to compensate for the loss of power flow over the interconnector.

Figure 4.11 shows a comparison between the no governor case and that with a governor on the synchronous generator in the South Australian network representation. A large difference can be seen when comparing the frequency responses. When the disturbance first causes a spike in frequency up to approximately 52.5 Hz, the frequency error is corrected and the frequency returns to the normal frequency operating band within 15 s when the governor is present. In the absence of the governor, the frequency only continues to rise. This is due to a slight change in the power output from the synchronous generator due to the presence of the governor. In each of these cases, the inverter behaviour is almost identical, as is the RMS voltage.

This result shows the importance of primary frequency control on the network stability, and how the removal of governors can have a detrimental effect. If too many governors are disabled within South Australia, it is more likely that instability will occur in the frequency if the Heywood Interconnector is tripped. It is likely that primary frequency control is needed to achieve optimal stability. More study is needed in this area.

4.5 Limitations

It should be noted that results may not accurately represent the South Australian network due to the simplified nature of the aggregate models of the synchronous generators and inverters. It therefore does not consider how synchronous generators may interact with each other. Synchronous generator parameters used in this model may also not reflect reality. The governor models on the synchronous generators also may not accurately reflect governor settings in the real network. Frequency dead bands have also not been included in the governor

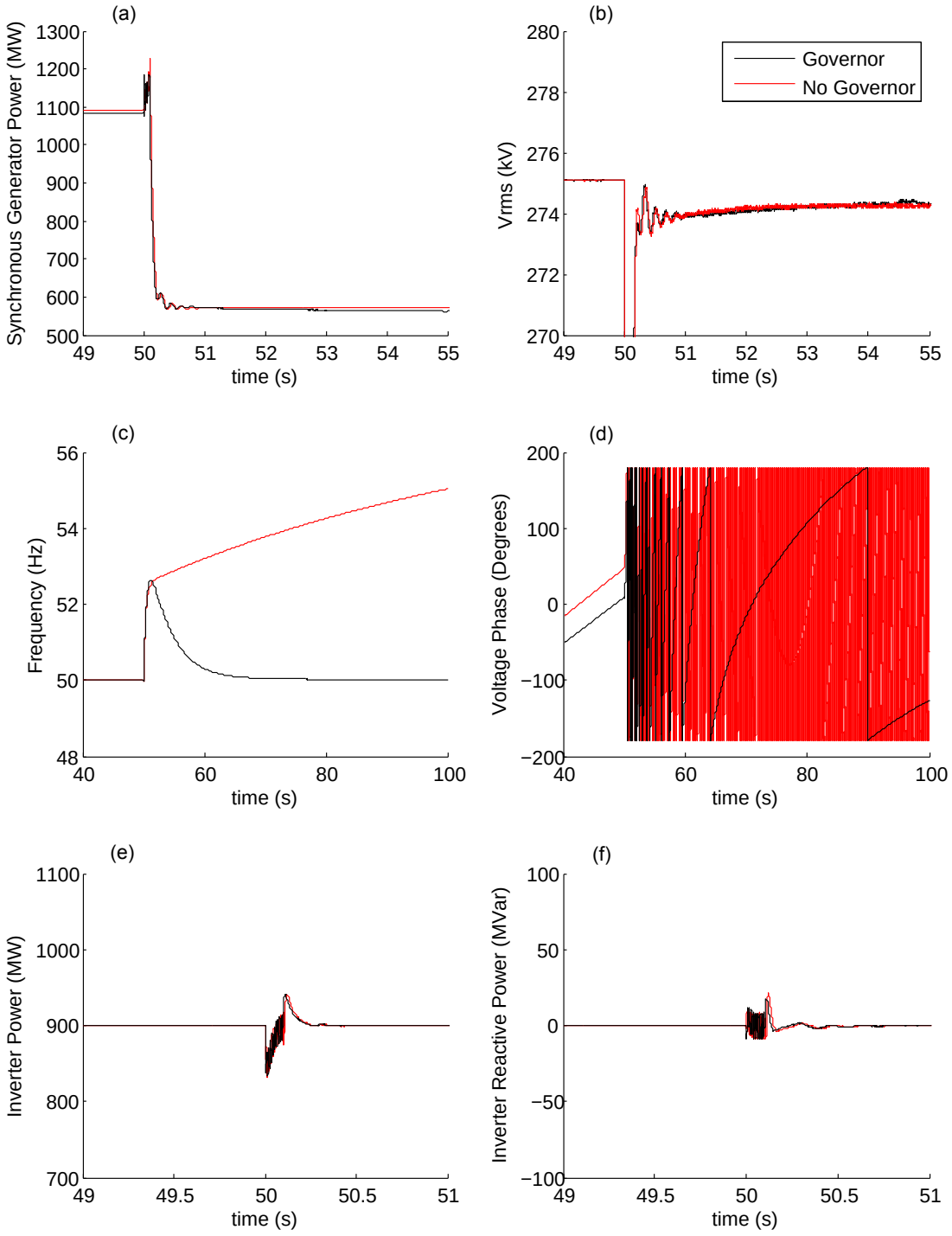

Figure 4.11 – Response after 100ms single phase to ground fault followed by an Interconnector trip in a network with a 900 MW inverter and 500 MW power flow across the Heywood Interconnector to Victoria. The figure shows (a) synchronous generator power (b) RMS line to line voltage (c) frequency (d) voltage phase angle (e) inverter power and (f) inverter reactive power in the presence (black) and absence (red) of a governor on the South Australian generator.

models in these simulations. The ability to increase the power generated from the synchronous machine in South Australia in simulations where the Heywood Interconnected is disconnected assumes the availability of adequate spinning reserve.

Loads are also modelled as aggregate loads, and do not include the complexity of real load behaviour. The effects of under frequency load shedding are not considered in this model either. For the sake of simplicity, there is also other equipment within the network that has not been included in the model, such as SVCs and STATCOMs for example.

This study also has not included the effects of a low short circuit ratio (SCR), which can occur in more remote locations where renewable generators may be located. It is also assumed that inverters in the network have access to readily available energy that can be accessed quickly. Many of these could be areas of further study. However, this is still a good starting point to look at this problem of mixed networks of inverters and synchronous generators.

4.6 Conclusions

In this Chapter, a simplified model of the South Australian electricity network, and its connection to Victoria across the Heywood Interconnector, is used to study the effect of the increasing penetration of inverter-based generation on network stability. The network, designed in PSCAD, is used to compare how different inverter penetration levels respond to disturbances in the network.

Firstly, a 100 ms single phase to ground fault is applied to the network. Very little difference is seen in the stability when the inverter penetration is changed. After this, simulations are run in which one of the two Heywood Interconnector lines are tripped. As before, it is shown that inverter penetration does not have much effect on the stability of the network. In the final simulation, both of the Heywood Interconnector lines are tripped, disconnecting South Australia from the rest of the grid. In this case, increasing the amount of inverter-based generation actually appears to improve the stability of the network.

These results assume the presence of governors on the synchronous generators in South Australia. Results indicate that the frequency stability of the network worsens without primary frequency control. While these simulations are done by simplifying the actual South Australian network and may be missing some of the complexities of the real network, these results are still useful. It indicates that increasing the amount of inverter-based generation within a network does not necessarily have a detrimental effect on stability, and may even improve it.

Chapter 5 will summarise the research that has been done in this thesis, present the conclusions, and provide recommendations for future work.

5 Conclusions

The increase in renewable generation within power networks has led to an increase in inverter-based generation along with a decrease in the proportion of power generated from synchronous generators, raising concerns about network stability. This thesis investigates the impact on the stability of a power network as asynchronous generation replaces synchronous generation.

The South Australian electricity network is used as a case study for studying the impact of inverter penetration on network stability. The South Australian network is chosen due to its relatively large proportion of renewable generation along with the fact that it has only one AC link joining it to the rest of the Australian network, the Heywood Interconnector. Recent events have also raised concerns about the stability of the South Australian network [42, 51]. For this reason, a simplified model of the South Australian network has been designed for study in PSCAD.

The network is designed with a synchronous generator and an inverter representing the aggregated synchronous and asynchronous generation within South Australia. The sizes of these generators can be varied to model different inverter penetration levels. The Heywood Interconnector is also included so that the power flow between South Australia and Victoria can be modelled. A large generator and load is used on the other side of the link to represent the electricity generated in eastern Australia.

Several types of inverter control systems are initially investigated. These include algebraic control, PI control of active and reactive power, as well as PI control of active power and voltage. Simulations are run at different levels of inverter penetration by altering the amounts of power generated by the synchronous generator and inverter in the PSCAD model. For each inverter power level, simulations are run using the three different types of inverter control mentioned above. A single phase to ground fault is introduced to the network in order to test the stability.

In the initial results, it is observed that the stability of the network generally decreases as inverter penetration level increases, with some exceptions. When comparing the different types of inverter control methods, both PI control of active and reactive power and algebraic control give much better responses than PI control of active power and voltage. More importantly, these initial results show that the inverter control needs a great deal of improvement. Large spikes, as well as a large amount of noise, are seen in both active and reactive power after the occurrence of the fault. In addition to improving the inverter control, a governor also needs to be added to the aggregate synchronous generator model in the South Australian network representation to more accurately model the behaviour of synchronous machines. These changes to the network are needed before any conclusions about network stability can be drawn.

A number of changes are made to the inverter to improve its design. As the PI inverter controls are initially only tuned using a trial and error approach, improvements need to be made so that these PI controllers can be better tuned. This is done for the PI control of active and reactive power, where the outer control loops controlling active and reactive power are improved by using better selected PI constants. The proportional and integral gains are optimised using the loop-shaping method. This is done by minimising the sum of errors between the desired open loop transfer function and the system open loop transfer function. Improvements to the inverter inner current control loop are also made by replacing the hysteresis current controller with a dq current controller.

Simulation results show a considerable improvement in the response of the inverter to disturbances, with much smaller spikes in real and reactive power and less oscillatory behaviour in response to the single phase fault. A governor is also designed for the South Australian synchronous generator. The design uses a PI based controller, with control of both frequency and power.

With these improvements, more accurate simulations can be run to test the stability of the network at differing levels of inverter penetration. To begin with, a single phase to ground fault is is applied. Increasing the power generated from the inverter relative to the power generated from the synchronous generator does not have a negative impact on stability. In fact, very little difference is seen in terms of stability at the different inverter penetration levels tested.

Following this, simulations are run in which one of the two Heywood Interconnector lines are tripped after a 100 ms single phase fault on one of the interconnector lines. Again, it is shown that inverter penetration does not have much effect on the stability of the network. Very similar responses are seen in both the voltage and frequency. To look at a more severe disturbance, a 120 ms two phase to ground fault is applied before the tripping of one of the interconnector lines. Again, these results show that increasing inverter penetration does not adversely affect the network stability.

Finally, the total disconnection of the Heywood Interconnector is studied, disconnecting South Australia from the rest of the Australian network. In these simulations, it is shown that

increasing the amount of inverter-based generation has a positive effect on the stability of the network. This is especially true for the frequency stability, where higher inverter penetrations showed less deviation from 50 Hz following the disturbance.

These results assume the presence of governors on the synchronous generators in South Australia, which may not be the case in reality. Simulations of a Heywood Interconnector trip are run, both with and without a governor on the aggregated South Australian synchronous generator representation. Frequency stability is shown to worsen when the governor is absent, highlighting the importance of primary frequency control.

Even though this analysis has been done using a simplified version of the actual South Australian network, and may be missing some of the complexities of the real network, these results are still useful. When inverters are utilising properly tuned controllers, they can have a positive effect on the stability of a network. These results indicate that increasing the amount of inverter-based generation within a network does not necessarily have a detrimental effect on stability, and may even improve it.

To summarise, the conclusions drawn based on simulations using the simplified South Australian network model are as follows:

- After tuning the inverter control using the loop-shaping method, simulation results show large improvements in the response of the inverter to disturbances
- Very little difference is seen in network stability at different inverter penetration levels in response to a single phase fault
- Increased inverter penetration does not adversely affect the network stability in response to a two phase fault followed by a line trip
- Increasing the amount of inverter-based generation has a positive effect on the stability of the network when simulating an interconnector trip
- Frequency stability is shown to worsen when the governor is absent, highlighting the importance of primary frequency control
- Overall, increasing the amount of inverter-based generation within a network does not necessarily have a detrimental effect on stability, and may even improve it

5.1 Future Work

In the PSCAD model for the South Australian electricity network used in this thesis, the aggregate synchronous generator model, representing all of the synchronous generation within South Australia, is controlled by a governor without any dead band. In reality, more and more generators are turning off their governors (or setting very wide dead bands) in order to

meet dispatch targets [44]. Further simulations could be performed to study what effect this has on the stability of the network. This could be done by having two or more synchronous generators in the South Australian PSCAD model, varying the proportion of synchronous generation with primary frequency control and subjecting the network to various disturbances. This could also be done at different levels of inverter penetration.

Another area for study is the impact of low SCR on network stability. With a fair number of renewable generators in remote locations behind long transmission lines and high impedance, recent discussion in Australia has brought up the issue of system strength in regards to low SCR levels [53]. This could perhaps be studied by altering the impedance to the inverter-based generator to study the stability of the network at various different SCR levels at the inverter.

It would also be useful to study the effect frequency control or virtual inertia on the inverter within the South Australian network model. This could be done in an attempt to further improve network stability at high inverter penetration levels.

A Appendix

A.1 Model Parameters

Table A.1 – South Australian Synchronous Machine Parameters

No. of Q-axis Damper Windings	2
Smoothing Time Constant to Exciter	0.015 s
Rated RMS Line-to-Neutral Voltage	9.24 kV
Rated RMS Line Current	72.17 kA
Inertia Constant	3.5 MWs/MVA
Neutral Series Resistance	1.0e4 pu
Neutral Series Reactance	0 pu
Iron Loss Resistance	300 pu
Armature Resistance [Ra]	0.003 pu
Potier Reactance [Xp]	0.15 pu
Unsaturated Reactance [Xd]	1.81 pu
Unsaturated Transient Reactance [Xd']	0.3 pu
Unsaturated Transient Time (Open) [Tdo']	8 s
Unsaturated Sub-Transient Reactance [Xd'']	0.23 pu
Unsaturated Sub-Transient Time (Open) [Tdo'']	0.03 s
Unsaturated Reactance [Xq]	1.76 pu
Unsaturated Transient Reactance [Xq']	0.65 pu
Unsaturated Transient Time (Open) [Tqo']	1 s
Unsaturated Sub-Transient Reactance [Xq'']	0.25 pu
Unsaturated Sub-Transient Time (Open) [Tqo'']	0.07 s
Air Gap Factor	1.0

Table A.2 – ST1A Exciter Parameters

Rate Feedback Gain [KF]	0.0 pu
Rate Feedback Time Constant [TF]	0.0 pu
Regulator Gain [KA]	200 pu
Regulator Time Constant [TA]	0.0 s
Maximum Regulator Output [VAMAX]	999 pu
Minimum Regulator Output [VAMIN]	-999 pu
Exciter Output Current Limit Reference [ILR]	4.4 pu
Exciter Output Current Limit Gain [KLR]	4.54 pu
Maximum Field Voltage [VRMAX]	7 pu
Minimum Field Voltage [VRMIN]	-6.4 pu
Field Current Commutating Impedance [KC]	0.04 pu
Upper Limit on Error Signal [VIMAX]	1.0e10 pu
Lower Limit on Error Signal [VIMIN]	-1.0e10 pu
Load Compensating Resistance [Rc]	0.0 pu
Load Compensating Reactance [Xc]	0.0 pu
Transducer Time Constant [Tr]	0.0 s
1st Lead Time Constant [TC]	0.0 s
1st Lag Time Constant [TB]	0.0 s
2nd Lead Time Constant [TC1]	0.0 s
2nd Lag Time Constant [TB1]	0.0 s

Table A.3 – PSS1A Power System Stabiliser Parameters

Transducer Time Constant [T6]	0.0 s
PSS Gain [Ks]	5.0 pu
Washout Time Constant [T5]	10.0 s
Filter Constant [A1]	0.0
Filter Constant [A2]	0.0
1st Lead Time Constant [T1]	0.0 s
1st Lag Time Constant [T2]	6.0 s
2nd Lead Time Constant [T3]	0.08 s
2nd Lag Time Constant [T4]	0.01 s
PSS Output Maximum Limit [VSTMAX]	0.1 pu
PSS Output Minimum Limit [VSTMIN]	-0.1 pu

Table A.4 – Wound Rotor Induction Machine Parameters

Rated Power	250 MVA
Rated Voltage (L-L)	275 kV
Base Angular Frequency	314.159 rad/s
Stator / Rotor Turns Ratio	2.638
Angular Moment of Inertia	0.7267 s
Mechanical Damping	0.01 pu
Stator Resistance	0.0054 pu
Wound Rotor Resistance	0.00607 pu
Magnetising Inductance	4.362 pu
Stator Leakage Inductance	0.102 pu
Wound Rotor Leakage Inductance	0.11 pu

Bibliography

[1] "South australian electricity report," report, AEMO, November 2017.

[2] R. Doherty, A. Mullane, G. Nolan, D. J. Burke, A. Bryson, and M. O'Malley, "An assessment of the impact of wind generation on system frequency control," *Power Systems, IEEE Transactions on*, vol. 25, no. 1, pp. 452–460, 2010.

[3] H. Dong, M. Jin, X. Ancheng, L. Tao, and Z. Guoqiang, "The uncertainty and its influence of wind generated power on power system transient stability under different penetration," in *Power System Technology (POWERCON), 2014 International Conference on*, pp. 675–680.

[4] J. Elizondo and J. L. Kirtley, "Effect of inverter-based dg penetration and control in hybrid microgrid dynamics and stability," in *Power and Energy Conference at Illinois (PECI), 2014*, pp. 1–6.

[5] F. Fernandez-Bernal, I. Egido, and E. Lobato, "Maximum wind power generation in a power system imposed by system inertia and primary reserve requirements," *Wind Energy*, vol. 18, no. 8, pp. 1501–1514, 2014.

[6] L. Meegahapola and D. Flynn, "Impact on transient and frequency stability for a power system at very high wind penetration," in *Power and Energy Society General Meeting, 2010 IEEE*, pp. 1–8.

[7] L. Yutian and L. Changgang, "Impact of large-scale wind penetration on transient frequency stability," in *Power and Energy Society General Meeting, 2012 IEEE*, pp. 1–5.

[8] J. Driesen and K. Visscher, "Virtual synchronous generators," in *Power and Energy Society General Meeting - Conversion and Delivery of Electrical Energy in the 21st Century, 2008 IEEE*, pp. 1–3.

[9] K. Visscher and S. W. H. de Haan, "Virtual synchronous machines (vsg's) for frequency stabilisation in future grids with a significant share of decentralized generation," in *SmartGrids for Distribution, 2008. IET-CIRED. CIRED Seminar*, pp. 1–4.

[10] W. Kuehn, "Control and stability of power inverters feeding renewable power to weak ac grids with no or low mechanical inertia," in *Power Systems Conference and Exposition, 2009. PSCE '09. IEEE/PES*, pp. 1–8.

[11] H. Alatrash, A. Mensah, E. Mark, R. Amarin, and J. Enslin, "Generator emulation controls for photovoltaic inverters," in *Power Electronics and Applications (EPE 2011), Proceedings of the 2011-14th European Conference on*, pp. 1–10.

[12] Z. Qing-Chang and G. Weiss, "Synchronverters: Inverters that mimic synchronous generators," *Industrial Electronics, IEEE Transactions on*, vol. 58, no. 4, pp. 1259–1267, 2011.

[13] K. Sakimoto, Y. Miura, and T. Ise, "Stabilization of a power system with a distributed generator by a virtual synchronous generator function," in *Power Electronics and ECCE Asia (ICPE & ECCE), 2011 IEEE 8th International Conference on*, pp. 1498–1505.

[14] S. M. Ashabani and Y. A. I. Mohamed, "A flexible control strategy for grid-connected and islanded microgrids with enhanced stability using nonlinear microgrid stabilizer," *Smart Grid, IEEE Transactions on*, vol. 3, no. 3, pp. 1291–1301, 2012.

[15] S. D'Arco and J. A. Suul, "Virtual synchronous machines - classification of implementations and analysis of equivalence to droop controllers for microgrids," in *PowerTech (POWERTECH), 2013 IEEE Grenoble*, pp. 1–7.

[16] S. D'Arco, J. A. Suul, and O. B. Fosso, "Control system tuning and stability analysis of virtual synchronous machines," in *Energy Conversion Congress and Exposition (ECCE), 2013 IEEE*, pp. 2664–2671.

[17] M. Ashabani and Y. A. R. I. Mohamed, "Integrating vscs to weak grids by nonlinear power damping controller with self-synchronization capability," *Power Systems, IEEE Transactions on*, vol. 29, no. 2, pp. 805–814, 2014.

[18] A. De Bonis, J. P. S. Catalao, A. Mazza, and G. Chicco, "A review on the dynamic analysis of weak distribution networks," in *Power Engineering Conference (UPEC), 2014 49th International Universities*, pp. 1–5.

[19] S. Rubino, A. Mazza, G. Chicco, and M. Pastorelli, "Advanced control of inverter-interfaced generation behaving as a virtual synchronous generator," in *PowerTech, 2015 IEEE Eindhoven*, pp. 1–6.

[20] M. Benidris and J. Mitra, "Enhancing stability performance of renewable energy generators by utilizing virtual inertia," in *Power and Energy Society General Meeting, 2012 IEEE*, pp. 1–6.

[21] P. Kundur, *Power System Stability and Control*. McGraw-Hill, 1994.

[22] P. Kundur, J. Paserba, V. Ajjarapu, G. Andersson, A. Bose, C. Canizares, N. Hatziargyriou, D. Hill, A. Stankovic, C. Taylor, T. V. Cutsem, and V. Vittal, "Definition and classification of power system stability ieee/cigre joint task force on stability terms and definitions," *IEEE Transactions on Power Systems*, vol. 19, pp. 1387–1401, Aug 2004.

[23] Y. ALShamli, N. Hosseinzadeh, H. Yousef, and A. Al-Hinai, "A review of concepts in power system stability," in *2015 IEEE 8th GCC Conference Exhibition*, pp. 1–6, Feb 2015.

[24] "Balancing and frequency control," report, NERC, 26 January 2011.

[25] "An introduction to australia's national electricity market," report, AEMO, July 2010.

[26] "Market ancillary services specification," report, AEMO, 01 May 2012.

[27] H. P. Beck and R. Hesse, "Virtual synchronous machine," in *Electrical Power Quality and Utilisation, 2007. EPQU 2007. 9th International Conference on*, pp. 1–6.

[28] E. W. Kimbark, *Power System Stability, Volume III Synchronous Machines*. 1956.

[29] M. Benidris, S. Elsaiah, S. Sulaeman, and J. Mitra, "Transient stability of distributed generators in the presence of energy storage devices," in *North American Power Symposium (NAPS), 2012*, pp. 1–6.

[30] J. Villena-Lapaz, A. Vigueras-Rodriguez, E. Gomez-Lazaro, A. Molina-Garcia, and J. A. Fuentes-Moreno, "Evaluation of frequency response of variable speed wind farms for reducing stability problems in weak grids," in *Power Electronics and Machines in Wind Applications (PEMWA), 2012 IEEE*, pp. 1–5.

[31] J. Morren, S. W. H. de Haan, W. L. Kling, and J. A. Ferreira, "Wind turbines emulating inertia and supporting primary frequency control," *Power Systems, IEEE Transactions on*, vol. 21, no. 1, pp. 433–434, 2006.

[32] P. BOUSSEAU, R. BELHOMME, E. MONNOT, N. LAVERDURE, D. BOËDA, D. ROYE, and S. BACHA, "Contribution of wind farms to ancillary services," report, CIGRE, 2006.

[33] J. Ekanayake and N. Jenkins, "Comparison of the response of doubly fed and fixed-speed induction generator wind turbines to changes in network frequency," *Energy Conversion, IEEE Transactions on*, vol. 19, no. 4, pp. 800–802, 2004.

[34] M. F. M. Arani and E. F. El-Saadany, "Implementing virtual inertia in dfig-based wind power generation," *Power Systems, IEEE Transactions on*, vol. 28, no. 2, pp. 1373–1384, 2013.

[35] X. Xinze, G. Hua, and Y. Geng, "Small signal stability of weak power system integrated with inertia tuned large scale wind farm," in *Innovative Smart Grid Technologies - Asia (ISGT Asia), 2014 IEEE*, pp. 514–518.

[36] Y. Xibo and L. Yongdong, "Control of variable pitch and variable speed direct-drive wind turbines in weak grid systems with active power balance," *Renewable Power Generation, IET*, vol. 8, no. 2, pp. 119–131, 2014.

[37] M. Swierczynski, R. Teodorescu, C. N. Rasmussen, P. Rodriguez, and H. Vikelgaard, "Overview of the energy storage systems for wind power integration enhancement," in *Industrial Electronics (ISIE), 2010 IEEE International Symposium on*, pp. 3749–3756.

[38] I. Egido, L. Sigrist, E. Lobato, L. Rouco, and A. Barrado, "An ultra-capacitor for frequency stability enhancement in small-isolated power systems: Models, simulation and field tests," *Applied Energy*, vol. 137, pp. 670–676, 2015.

[39] "South australian electricity report," report, AEMO, August 2016.

[40] High Voltage Network Main System Diagrams, https://www.aemo.com.au/media/Files/Other/planning/NEMSLDs2015V3.pdf, accessed 2018-25-01.

[41] "Renewable energy integration in south australia," report, AEMO, Electranet, October 2014.

[42] "Black system south australia 28 september 2016," final report, AEMO, March 2017.

[43] K. Summers, "Fast frequency service - treating the symptom not the cause," 2017.

[44] "Summary of digsilent investigation into frequency control in the nem under normal conditions," report, AEMO, August 2017.

[45] PSCAD Homepage, https://hvdc.ca/pscad/, accessed 2017-06-29.

[46] "Ieee recommended practice for excitation system models for power system stability studies," *IEEE Std 421.5-1992*, 1992.

[47] "Generator fault ride through (frt) investigation," report, Transpower, February 2009.

[48] "Power system frequency and time deviation monitoring report - reference guide," report, AEMO, 2 July 2012.

[49] Frequency-Domain Robust Control Toolbox, http://la.epfl.ch/FDRC_Toolbox, accessed 2017-10-12.

[50] MathWorks, "Hydraulic turbine and governor." https://au.mathworks.com/help/physmod/sps/powersys/ref/hydraulicturbineandgovernor.html;jsessionid=146b1b63b6a136f9c860e953ec59, accessed 2017-06-17.

[51] "Final report - south australia separation event, 1 december," report, AEMO, 28 February 2017.

[52] AEMC, "National electricity rules," 2018.

[53] "South australian system strength assessment," report, AEMO, September 2017.